Article

Not peer-reviewed version

The Role of CD68+ Cells in Bronchoalveolar Lavage Fluid for the Diagnosis of Respiratory Diseases

Igor D. Zlotnikov , Natalia I. Kolganova , Shamil A. Gitinov , Dmitry Y. Ovsyannikov , Elena V. Kudryashova *

Posted Date: 7 August 2025

doi: 10.20944/preprints202508.0471.v1

Keywords: CD68+ macrophages; bronchoalveolar lavage fluid (BALF); respiratory diseases; liposome-based assay; confocal laser scanning microscopy (CLSM); FTIR spectroscopy; diagnostic fingerprinting; cell analysis

 doi:10.20944/preprints202508.0471.v1

Article

The Role of CD68+ Cells in Bronchoalveolar Lavage Fluid for the Diagnosis of Respiratory Diseases

Igor D. Zlotnikov [1], Natalia I. Kolganova [2,3], Shamil A. Gitinov [2,3], Dmitry Y. Ovsyannikov [2,3] and Elena V. Kudryashova [1,*]

[1] Faculty of Chemistry, Lomonosov Moscow State University, Leninskie Gory, 1/3, 119991 Moscow, Russia
[2] State Budgetary Healthcare Institution of the Moscow City Department of Health Morozovskaya Children's City Clinical Hospital, 119049 Moscow, Russia, 1/9 4th Dobryninsky Lane
[3] Federal State Autonomous Educational Institution of Higher Education "Patrice Lumumba Peoples' Friendship University of Russia", 6, Miklukho-Maklaya str., 117198 Moscow, Russia
* Correspondence: helenakoudriachova@yandex.ru

Abstract

Addressing the critical challenge in the differential diagnosis of severe inflammatory lung diseases, we propose a novel methodology for the analysis of macrophage surface receptors, CD68 and CD206, using specific non-antibody ligands. We aimed to develop a non-antibody alternative for the fluorometric detection of CD68+ cells, focusing on macrophages as key functional markers in inflammatory processes. Our marker based on dioleylphosphatidylserine (DOPS), a specific ligand to CD68, incorporated into a liposomal delivery system. The specificity of this DOPS-based ligand can be precisely modulated by the liposome's composition and the polyvalent presentation of the ligand. We synthesized a series of fluorescently-labeled DOPS-based ligands and developed a liposome-based sandwich fluorometric assay. This assay enables the isolation and quantification of CD68 receptor presence from bronchoalveolar lavage fluid (BALF). The results confirmed the specific binding of DOPS/lecithin liposomes to CD68+ cells compared to control lecithin systems. Furthermore, the incorporation of PEGylated 'stealth' liposomes significantly enhanced binding specificity and facilitated the generation of distinct binding profiles, which proved valuable in differentiating various inflammatory conditions. This approach yielded unique binding profiles of PS-based ligands to CD68+ cells, which varied significantly among a broad range of respiratory conditions, including primary ciliary dyskinesia, bronchial asthma, bronchitis, bacterial infection, pneumonia, and bronchiectasis. Confocal Laser Scanning Microscopy demonstrated selective binding and intracellular localization of the DOPS-based marker within CD68+ macrophages from BALF samples of patients with bronchitis or asthma. Fourier-transform infrared (FTIR) spectroscopy has revealed changes in characteristic bands of the FTIR spectra upon binding of DOPS-based marker with CD68+ cells, providing a quantitative measure of binding parameters and potentially able to differentiate between CD68+ cells subtype profile. The binding parameters of this multivalent composite ligand with the CD68 receptor are comparable to those of antibodies. This suggests that for certain *in vitro* diagnostic applications (e.g., BALF analysis in bronchial asthma), where the cellular diversity is limited, the inherent binding specificity of phosphatidylserine may offer a sufficient and viable alternative to conventional antibodies. Our results demonstrate the remarkable potential of this novel approach for the developing non-antibody-based systems for the differential diagnosis of the respiratory diseases.

Keywords: CD68+ macrophages; bronchoalveolar lavage fluid (BALF); respiratory diseases; liposome-based assay; confocal laser scanning microscopy (CLSM); FTIR spectroscopy; diagnostic fingerprinting; cell analysis

 doi:10.20944/preprints202508.0471.v1

1. Introduction

Severe inflammatory pulmonary diseases represent an escalating global health burden, tragically claiming infant lives due to underdeveloped respiratory systems and silent progression, while in adults, they precipitate devastating complications such as cytokine storms (as witnessed in COVID-19 [1]), irreversible fibrosis in conditions like chronic obstructive pulmonary disease (COPD) [2], and profound reductions in quality of life. Current diagnostic paradigms, reliant on clinical presentation and systemic blood analyses, are demonstrably inadequate in precision and, crucially, fundamentally fail to provide prognostic insights into the risk of life-threatening complications. While bronchoalveolar lavage (BAL) is a widely established method for respiratory tract examination [3], particularly when critical states are anticipated, its full diagnostic potential remains untapped. It is within this urgent context that our central thesis emerges: to comprehensively investigate the pivotal role of CD68+ cells—including macrophages, where CD68 is prominently expressed (CD68, a transmembrane protein weighing 101 kDa), and their functionally intertwined eosinophils (given the established co-occurrence and influence of macrophage CD68 activity on eosinophil-driven pathology)—as dynamic biomarkers for both inflammation development and exquisitely precise diagnostic and prognostic stratification of these complex respiratory disorders. Analysis of the BAL fluid cellular composition directly from the alveolar space of the lungs of the is crucial for detecting pathological processes in the lungs [4–7].

Macrophages "govern" inflammatory processes, with the delicate balance of their subpopulations critically determining disease progression and resolution. Our recent, in-depth investigation into macrophage receptors and their specific ligands has unveiled a groundbreaking insight: we discovered not merely discrete M1/M2 subsets, but a continuous spectrum of macrophage subpopulations, profoundly differing in receptor distribution and, consequently, in their capacity to bind diverse carbohydrate-containing ligands. To precisely map this previously unrecognized depth of functional heterogeneity, we developed a unique suite of fluorescently labeled specific ligands—acting as sophisticated antibody surrogates—which, when applied to patient BALF, consistently revealed that each distinct pulmonary disease manifests a characteristic 'fingerprint' of ligand binding to immune cells [8–10].

By analyzing CD68, a key receptor found on all macrophages, we gain insights into macrophage functioning. Crucially, this also helps us understand the broader inflammatory state and the functional role of other immune cells, particularly eosinophils, as macrophage CD68 activity is frequently linked to eosinophil involvement in many respiratory diseases. Both CD68+ macrophages and eosinophils play an important role in the pathogenesis of a wide range of respiratory diseases, including asthma, COPD, interstitial lung disease (ILD), allergic rhinitis, and other conditions [11–14] (Table 1). Elevated levels of eosinophils in the BAL fluid are a characteristic feature of asthma in both children and adults [15]. In acute eosinophilic pneumonitis (AEP), a rare and severe condition characterized by rapid accumulation of eosinophils in the alveoli, BAL fluid analysis reveals a significant increase in their number [16–18].

Table 1. The role of eosinophils in pulmonary diseases, their treatment, and the typical percentage of eosinophils in bronchoalveolar lavage fluid.

Respiratory Disease	Typical Eosinophil % in BAL	Role of Eosinophils	Treatment	References
Healthy	<1%	Eosinophils protect the body from toxins, allergens, and multicellular parasites. Destruction of multicellular parasites.	–	[19,20]

 doi:10.20944/preprints202508.0471.v1

Asthma (Eosinophilic Phenotype)	> 2%	Key effector cells in Type 2 inflammation, contribute to airway inflammation, hyperresponsiveness, and remodeling.	Inhaled corticosteroids, bronchodilators, biologics (e.g., anti-IL-5, anti-IL-4/13) for severe cases.	[15,21–23]
Acute Eosinophilic Pneumonia (AEP)	Typically > 15%	Accumulation in alveolar spaces and interstitium leading to acute lung injury.	Systemic corticosteroids (rapid and dramatic response).	[16–18]
Chronic Eosinophilic Pneumonia (CEP)	Often > 30% (can be 12-95%)	Infiltration of pulmonary interstitium and alveoli, contributing to chronic inflammation and lung opacities.	Systemic corticosteroids (often prolonged course due to high relapse rate), sometimes corticosteroid-sparing agents.	[24–26]
Allergic Bronchopulmonary Aspergillosis (ABPA)	Peripheral blood eosinophilia (not essential for diagnosis)	Mediators of allergic inflammation in response to *Aspergillus fumigatus*, contribute to mucus plugging and bronchiectasis.	Systemic corticosteroids, antifungals (e.g., itraconazole), sometimes biologics.	[27–29]
Eosinophilic Granulomatosis with Polyangiitis (EGPA)	>10%	Contribute to tissue damage through granule protein release, involved in vasculitis and granuloma formation.	Systemic corticosteroids, immunosuppressants (e.g., cyclophosphamide, azathioprine), biologics (e.g., mepolizumab).	[30–32]
Chronic Obstructive Pulmonary Disease (COPD)	Can be mildly elevated	In a subset of patients, may contribute to airway inflammation and exacerbations; their precise role is still under investigation.	Bronchodilators, inhaled corticosteroids (especially in those with higher eosinophil counts), pulmonary rehabilitation.	[2,33–36]

Functional diversity of eosinophils is manifested both in their proinflammatory activity and in their involvement in tissue remodeling and other processes [19]. Determining the level of eosinophils in BALF in the amount of more than 5% of the differential count of leukocytes indicates the presence of a pathological process in the lungs. In eosinophilic lung diseases, the proportion of eosinophils in the BAL fluid can be >10% or more (Table 1). Thus, the quantitative determination of eosinophils in the BAL fluid is an important element in the diagnosis of many respiratory diseases, especially those characterized by eosinophilic inflammation.

Given the close relationship (in terms of coexistence and complementary action) of CD68+ macrophages with eosinophils [37–41], especially in eosinophilic asthma, and the functional uniqueness of M1/M2 macrophage phenotypes, a comprehensive diagnostic approach is needed. Simultaneous typing of CD68+ macrophages and assessment of the contribution of eosinophils, supplemented by CD206+ cell analysis to determine the specific roles of macrophages, provide accurate data for the diagnosis of diseases. It has been shown that CD68+ macrophages can engage in interactions eosinophils, affecting their function through, for instance, the release of chemokine CCL24 [37], which elicit the migration of eosinophils towards the respiratory tract.

This research addresses to explore the role and analytical significance of CD68+ cells in differential diagnosis of the respiratory disorders and the creation of a liposome-based assay using a phosphatidylserine (PC)-based marker for CD68+ cells. We developed a novel approach leveraging DOPS (dioleoylphosphatidylserine) as a specific ligand for CD68 receptor [38,42]. Our methodology

 doi:10.20944/preprints202508.0471.v1

includes precisely engineered DOPS/lecithin liposomes of different compositions, fluorescently labeled with Rhodamine 6G (R6G), for the sensitive and specific typing of CD68+ cells in BALF. The precise identification and quantification of both CD68+ macrophages and their co-occurring eosinophils in BALF, facilitated by this innovative system, promise to yield invaluable insights into the intricate mechanisms of specific respiratory inflammatory processes.

2. Materials and Methods

2.1. Reagents

Dioleoyl phosphatidylserine (DOPS) was purchased from Chimmed (Moscow, Russia). Lecithin from soybeans was purchased from Reachim (Moscow, Russia). 4′,6-diamidino-2-phenylindole (DAPI) and rhodamine 6G (R6G) was purchased from Sigma Aldrich (St. Louis, MO, USA).

2.2. Ethical Approval and Sample Collection

BALF samples were obtained from the Morozovskaya Children's City Clinical Hospital following patient consent and strict adherence to ethical guidelines. Cellular components from bronchoalveolar lavage fluid (BALF), were selectively enriched through a dual approach, combining conventional histological methodologies with a novel, lipid-based capture strategy. This innovative method specifically targets CD68-expressing cells by leveraging the inherent binding properties of dioleoylphosphatidylserine (DOPS) as a ligand. The methodology commences with the precise fabrication of lipid films, composed of either DOPS/lecithin or lecithin, typically via solvent evaporation, to form robust capture surfaces. Subsequently, the heterogeneous BALF cell suspension is introduced and incubated for 60 minutes at 37°C, facilitating selective adhesion of target cells.

For this, cell suspensions were prepared by cytocentrifugation using an Eppendorf centrifuge, then stained with a Romanowsky stain for clear morphological differentiation. Subsequently, differential cell counts were performed under a light microscope at high magnification.

2.3. Liposome Preparation and Characterization

A range of liposomal formulations were prepared to investigate the cellular interactions of different lipid compositions. These included:

- Lecithin-based liposomes: Pure lecithin liposomes served as a control formulation.
- Dioleoyl phosphatidylserine (DOPS) / Lecithin liposomes: Liposomes were prepared with varying ratios of DOPS to lecithin (25/75, 50/50, and 75/25 w/w) to explore the influence of anionic lipid content on cellular uptake.
- PEGylated Stealth Liposomes: To impart stealth properties and potentially prolong circulation time, DOPS/lecithin liposomes (specifically the 75/25 w/w ratio was used for these, though you can specify if others were PEGylated) were further functionalized with DSPE-PEG_{2000} at varying concentrations (1–33 mass%).

For all liposome preparations, the respective lipids (lecithin, DOPS, and DSPE-PEG2000 where applicable) were initially dissolved in ethanol at a final lipid concentration of 10 mg/mL (for binary formulations, e.g., lecithin or DOPS/lecithin 50/50, the specified concentrations were used). The solvent was then removed by rotary evaporation, followed by drying under a gentle stream of air to ensure complete residual solvent removal, yielding a thin lipid film.

These dried lipid films were subsequently hydrated with either PBS or PBS containing the encapsulated fluorescent dye R6G. Samples were further treated in a water bath sonicator to ensure complete dispersion and to potentially reduce vesicle aggregation. Then, rehydrated lipid dispersions were then subjected to extrusion through polycarbonate membranes with a pore size of 200 nm. This process was performed to achieve a defined and uniform liposome size distribution. Unencapsulated R6G was separated from the liposomal formulations via dialysis using a dialysis

 doi:10.20944/preprints202508.0471.v1

membrane with a 3 kDa molecular weight cut-off (MWCO). The dialyzed liposomes were then collected.

2.4. Liposome-Based Sandwich Assay for CD68 Receptor Quantification

A novel, lipid-film based assay was meticulously developed for the selective capture and quantitative analysis of CD68-positive macrophages and eosinophils from heterogeneous cellular suspensions. Briefly, a cell suspension derived from BALF was introduced onto pre-fabricated lipid films in wells of 96-well clear bottom Costar plate. These films, consisting of either dioleoyl phosphatidylserine (DOPS)/lecithin or lecithin-only (serving as a control for non-specific binding), were prepared with *in situ* encapsulated rhodamine 6G (R6G) to enable fluorescent detection. The cell suspensions were then incubated with the lipid films at a physiological temperature of 37°C for a standardized period of 60 minutes. This incubation facilitated the specific interaction between the surface-exposed CD68 receptors on target cells and the complementary lipid components within the DOPS/lecithin films. Following incubation, non-adherent cells were meticulously dislodged and removed through two sequential washing steps with phosphate-buffered saline (PBS), ensuring the isolation of only bound cellular populations. The successfully captured CD68-positive cells, now associated with the DOPS/lecithin films pre-loaded with R6G, were subsequently visualized and quantified using fluorimetry and fluorescence microscopy. The intensity of the fluorescent signal emitted by the R6G served as a direct quantitative measure, linearly correlating with the number of specifically bound liposomes and, by extension, the abundance of CD68-positive cells. Lecithin-only lipid films, devoid of DOPS and R6G, were employed as a crucial control to determine the extent of non-specific cellular adsorption and to enable accurate background fluorescence subtraction. The binding kinetics of R6G-labeled lecithin-based and DOPS/lecithin-based liposomes to eosinophils in BALF samples from patients with various respiratory conditions were assessed. Measurements were performed with $5x10^5$ cells per well, a lipid concentration of 0.1 mg/mL, and R6G concentration of 1 μg/mL in PBS (0.01M, pH 7.4) at 37 °C. Normalized kinetic curves of R6G fluorescence changes were recorded over time on SpectraMax M5 (Molecular Devices, CA, USA).

2.5. Confocal Laser Scanning Microscopy (CLSM) Analysis

BALF samples from patients with bronchial asthma and acute bronchitis were incubated with R6G-labeled lecithin-based and DOPS/lecithin-based liposomes. Eosinophils were visualized using CLSM (Olympus FluoView FV1000), with nuclei stained with DAPI. DAPI fluorescence was detected at $\lambda_{exci,max}$ = 340 nm, λ_{emi} = 410-500 nm. R6G fluorescence was detected at $\lambda_{exci,max}$ = 520 nm, λ_{emi} = 570-700 nm. Integral values of fluorescence signal intensity, background intensity, signal-to-background ratio, and co-localization of R6G with DAPI were calculated using ImageJ software (1.54d).

2.6. FTIR Spectroscopy Analysis

To validate binding specificity, FTIR spectroscopy was employed to analyze interactions between liposomes and eosinophils isolated from BAL samples of patients with bronchial asthma using Bruker TensorFlow 27 device (Bruker, Ettlingen, Germany) and MICRAN-3 FTIR microscope (Simex, Novosibirsk, Russia). Spectra of cells (eosinophils and CD68+ macrophages) were obtained at different time points (step 5 min) during incubation with R6G-loaded lecithin-based or DOPS/lecithin-based liposomes in PBS (0.01M, pH 7.4) at 37 °C. Analysis focused on the amide I region (1600-1700 cm^{-1}) and the $\nu(CH_2)$ region (2800-3000 cm^{-1}). Kinetic curves of FTIR peak positions for Amide I (maximum position and intensity) and $\nu(CH_2,s)$ and $\nu(CH_2,as)$ (maximum positions) were generated as a marker of liposome-cell interaction.

2.7. Evaluation of Assay Performance and Clinical Correlation

To rigorously assess the diagnostic potential and clinical relevance of the developed lipid-film based capture assay, its performance was evaluated using patient-derived samples. Two key

 doi:10.20944/preprints202508.0471.v1

quantitative parameters were determined for both the experimental (DOPS/lecithin) and control (lecithin-only) liposome formulations: the initial binding rate (expressed as %/min), reflecting the kinetics of cellular capture, and the overall effective binding index after a 1-hour incubation period (expressed as %), indicating the total cellular capture efficiency.

Measurements were conducted on BALF samples obtained from a carefully selected cohort of six distinct patients. These patients were chosen to represent a diverse spectrum of clinical diagnoses, thereby enhancing the generalizability of the findings regarding the utility of this assay across varying pathological conditions. For each patient sample, all binding parameters were meticulously assessed in triplicate (N=3 independent technical replicates) to ensure statistical robustness and reproducibility. Subsequently, these newly derived liposome-binding indices were correlated against established clinical biomarkers, including comprehensive complete blood count (CBC) parameters and C-reactive protein (CRP) levels, to investigate their potential as novel diagnostic indicators reflective of underlying disease states or inflammatory processes.

3. Results and Discussion

3.1. CD68+ Cells Isolation Technique and CD68 Validation

We have developed a novel, specific and effective approach for the direct analysis of CD68+ immune cells, primary macrophages, crucial for understanding respiratory inflammatory processes. We suggest applying a series of fluorescently labeled liposomal ligands based on phosphatidylserine (PS), specifically dioleylphosphatidylserine (DOPS) as a primary, high-affinity ($K_d \approx 10^{-7}$ M) ligand for CD68. This strategy leverages the inherent binding properties of DOPS, enabling its use as a powerful, antibody-independent alternative for routine *in vitro* diagnostics in cellularly limited samples, such as BALF.

The base of our approach involves DOPS/lecithin liposomes as convenient, self-assembling forming lipid carriers (Figure 1a). These liposomes contain fluorescent reporters like Rhodamine 6G, forming a tunable system where specificity can be regulated through the ligand's content and architecture. The remarkable specificity of DOPS binding is rooted in CD68's well-established role as a scavenger receptor, whose three-dimensional structure reveals distinct hydrophobic pockets ideally suited for binding anionic phospholipids like DOPS.

The protocol includes the preparation of DOPS/lecithin film at the bottom of a fluorescent plate (1), through solvent evaporation techniques. These films create capture layers (2a). BALF, containing a heterogeneous population of CD68+ cells including macrophages and eosinophils, is then added and incubated at 37 °C for 1 hour to facilitate interaction between CD68 receptors on the target cells and the DOPS ligands in films (2b). Washing steps (2c) remove unbound cells, leaving only CD68+ cells interacting with the DOPS/lecithin liposomes (different composition) containing R6G (2d). This interaction is specific, mediated by the phospholipid DOPS. Finally, the captured CD68+ cells are visualized via fluorescence microscopy (3) by detecting the emitted fluorescence of R6G incorporated within the liposomes bound to CD68+ cells. The changes in the intensity of the fluorescent signal (binding index relative to control) are directly correlated with the content of DOPS/lecithin liposomes bound to CD68+ cells. Lecithin-based liposomes without DOPS were used as a control, and serve to assess non-specific binding of liposomes to the cells.

 doi:10.20944/preprints202508.0471.v1

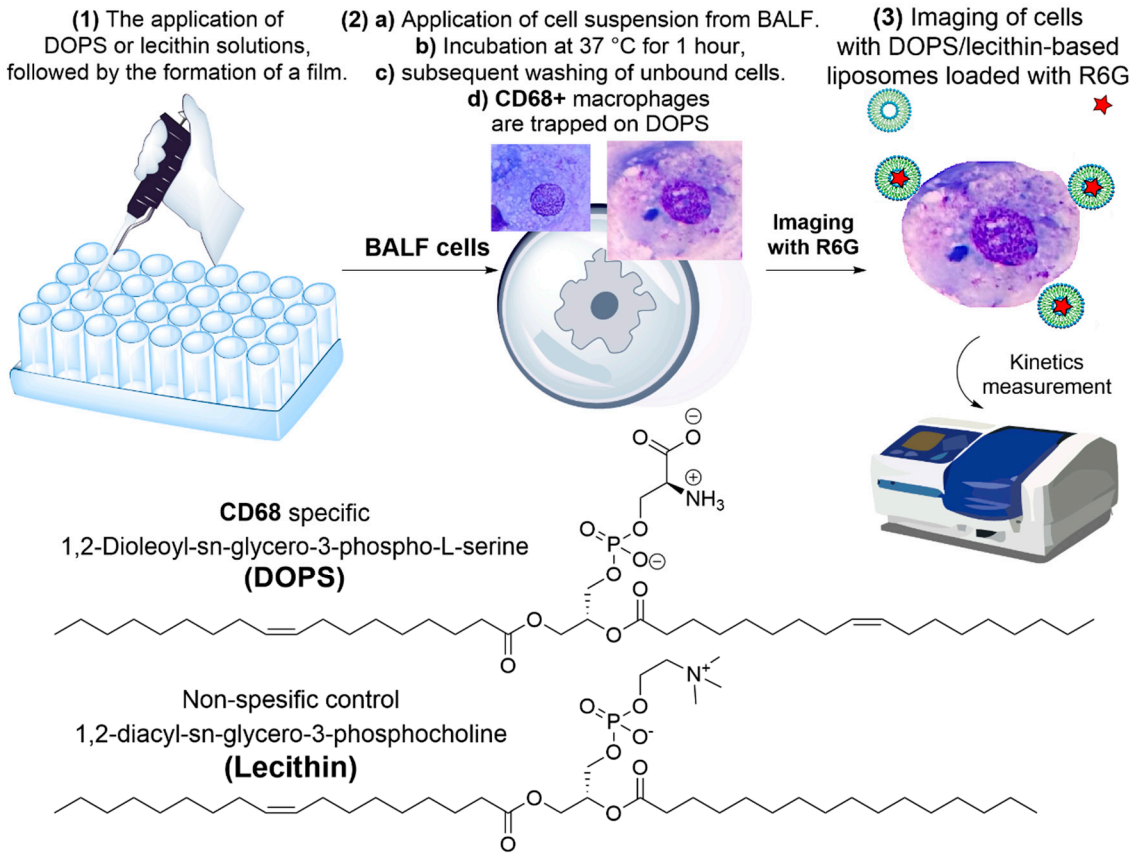

(a)

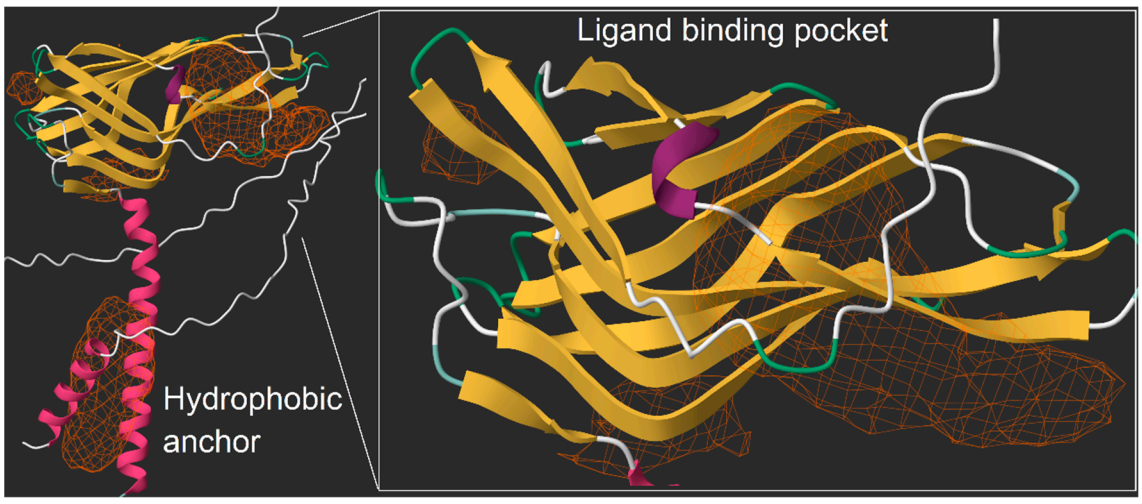

(b)

Figure 1. (a) Schematic representation of the process of isolating eosinophils from BALF and subsequently typing them using the sandwich technique of analysis for receptors CD68, which are visualized using liposomes based on DOPS/lecithin loaded with R6G. (b) Predicted three-dimensional structure of CD68 protein in alpha format (UniProt P34810) and the location of the hydrophobic anchor for protein attachment to the membrane and zoomed hydrophobic pockets for ligand binding (LDL, cell residues, DOPS, etc.). The hydrophobic pockets are indicated by a grid.

Figure 1b presents the predicted three-dimensional structure of the human CD68 protein (UniProt P34810), offering crucial structural insights into its function. A prominent feature highlighted is the hydrophobic anchor, vital for the protein's stable integration into the cell membrane, reflecting its role as a surface-expressed receptor. Furthermore, the structure reveals

 doi:10.20944/preprints202508.0471.v1

distinct hydrophobic pockets. These pockets are essential for the interaction with a diverse range of ligands, encompassing oxidized low-density lipoproteins (LDL) that are specifically targeted due to their origin as byproducts of cellular degradation. CD68 serves as a receptor-like scavenger, recognizing and binding to these ligands, including cellular debris, and specifically, anionic phospholipids like DOPS (dioleoylphosphatidylserine). This structural depiction supports CD68's established role as a scavenger receptor involved in the recognition and internalization of diverse extracellular materials, providing a basis for understanding its interaction with specific liposomal formulations and model lipid films containing DOPS.

To further quantify these interactions, computational analysis was performed using the open-access platform (open.playmolecule.org) to predict the binding affinity of CD68 with DOPS and lecithin. DOPS exhibits a more favorable (more negative) binding free energy (ΔG) of –9.7 kcal/mol and a higher predicted pK_d of 7.2, compared to lecithin's ΔG of –8.1 kcal/mol and pK_d of 6.0. This computational finding indicates a significantly stronger predicted binding affinity of CD68 for DOPS than for lecithin (selectivity is more than 10 times). This aligns with CD68's well-documented function as a scavenger receptor that preferentially recognizes and binds to anionic phospholipids like phosphatidylserine (PS), which is widely exposed on the surface of apoptotic cells to facilitate their clearance. Lecithin (phosphatidylcholine, PC), being a zwitterionic lipid, would consequently be expected to interact less strongly.

The remarkable specificity of our DOPS-based liposomes for the CD68 receptor arises from a sophisticated interplay of biophysical forces. We've identified three primary factors that contribute to this highly selective binding (Figure S1):

1. **Electrostatic complementarity (Major factor):** At the core of this selectivity lies electrostatic complementarity. Detailed analysis of the CD68 receptor's surface reveals a distinct region characterized by a concentrated positive charge, primarily due to the presence of arginine and lysine residues. Phosphatidylserine (DOPS), in turn, possesses a net negative charge on its headgroup. This fundamental charge difference drives a powerful electrostatic attraction, facilitating the formation of robust ionic bonds, or 'salt bridges,' with CD68's positively charged pocket. In contrast, lecithin, being zwitterionic (with a net neutral charge), lacks the focused negative charge required for such strong, directed ionic interactions. Furthermore, its positively charged moiety can experience electrostatic repulsion from the CD68 binding site.
2. **Geometric and steric contributions:** Beyond charge, geometric fit plays a crucial role. The headgroup of DOPS is notably more compact, with a cross-sectional area of approximately 65.3 Å^2. Conversely, the lecithin headgroup is bulkier, measured at around 72.5 Å^2. This smaller footprint of the DOPS headgroup allows it to fit more precisely and deeply into the CD68 binding pocket, effectively minimizing steric hindrance and maximizing the number of favorable molecular contacts. This optimal fit enhances the overall binding affinity and specificity.
3. **Hydrophobic interactions and a universal recognition mechanism:** While the primary specificity is determined by the polar headgroup interactions, the overall affinity to lipid structures is significantly enhanced by the hydrophobic tails of the phospholipids. These tails engage with a complementary hydrophobic channel within the CD68 receptor, providing a substantial contribution to the binding energy for both DOPS and lecithin.

Importantly, this mechanism of recognizing negatively charged motifs appears to be a universal function for CD68. It explains why CD68 effectively binds not only phosphatidylserine presented on apoptotic cells but also oxidized low-density lipoproteins (oxLDL). During the oxidation process, oxLDL acquires negatively charged groups on its surface, which are recognized by the very same positively charged pocket on CD68. This phenomenon strongly reinforces CD68's critical role as a versatile pattern recognition receptor for various danger-associated molecular patterns (DAMPs), highlighting its significance in innate immunity and inflammatory responses. These *in silico* predictions provide a molecular basis for understanding the selective interactions observed in experimental systems, reinforcing the potential for targeted delivery strategies leveraging CD68.

 doi:10.20944/preprints202508.0471.v1

3.2. CD68+ Macrophages, Eosinophils and Other Cells in BALF Characterization

According to the available literature, cells that express the CD68 receptors exhibit characteristics mainly associated with the pro-inflammatory M1 macrophage phenotype, whereas cells bearing the CD206 antigen mainly display an anti-inflammatory profile [43]. BALF comprises a heterogeneous population of cells reflecting the underlying pulmonary condition. Figure 2 demonstrates this cellular heterogeneity, showing macrophages, eosinophils, neutrophils, and epithelial cells (2a, 2b). Our analysis focused on isolating specific target cells (2c), primarily macrophages, for subsequent CD68 receptor analysis.

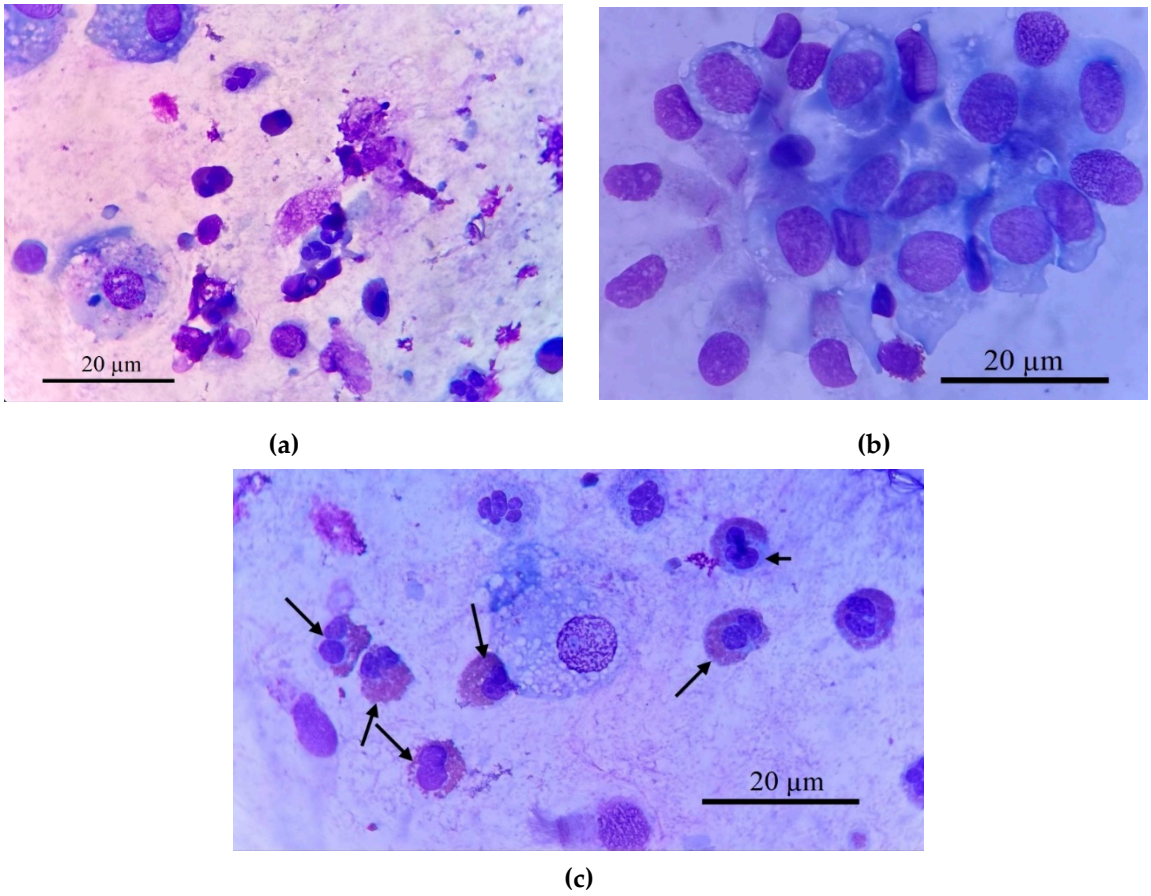

Figure 2. Micrographs of cells from BALF samples of a patient with bronchial asthma (1 sample): (a) macrophages, eosinophils, neutrophils, (b) epithelial cells, (c) The target CD68+ macrophages are depicted in the center, and eosinophils with arrows indicating.

Figure 2 provides representative micrographs illustrating the heterogeneous cellular composition of BALF samples from a patient with bronchial asthma. Histological characterization, employing Romanowsky staining, revealed distinct cell populations critical to understanding respiratory inflammation. **Macrophages** (Figure 2a, 2c) are typically identified by their large size, abundant cytoplasm, and often a lobed nucleus. Within this population, a significant subtype are **epithelioid cells** (Figure 2b), as one of the type of differentiated macrophages with pronounced secretory activity characteristic of M1-phenotype reflecting an active inflammatory response [44]. These cells often lacking phagosomes, and possess a well-defined lobed nucleus with a prominent nucleolus. A hallmark morphological feature of epithelioid cells is their characteristic "lacy" irregular plasma membrane edge, resulting from continuous vesicle fusion, and they can reach sizes up to 100 µm, frequently containing 2-3 lobed nuclei. Their presence, alongside elevated pro-inflammatory cytokines such as IL-8 (and to a lesser extent IL-2 and IL-1β) and decreased IL-4 and IL-5, strongly

 doi:10.20944/preprints202508.0471.v1

indicates a predominance of M1-phenotype macrophages, reflecting an active inflammatory response.

Eosinophils (indicated by arrows in Figure 2c, also visible in 2a) are readily distinguishable by their bilobed or trilobed nucleus and, most characteristically, their cytoplasm filled with numerous distinct, bright reddish-orange granules when stained with Romanowsky dyes. **Neutrophils** (Figure 2a) exhibit a multi-lobed nucleus and pale, fine granules. This detailed cellular analysis allows for comprehensive assessment of inflammatory profiles in respiratory diseases.

The Table 2 summarizes the differential cell counts obtained from BALF samples of several patients representing various respiratory diseases. These data highlight the distinct cellular profiles characteristic of each condition.

Table 2. Cellular composition of studied BALF from patients with various diagnoses.

Disease	Neutrophils (%)	Monocytes (%)	Lymphocytes (%)	Eosinophils (%)	Macrophages (%)	Other Observations
Eosinophilic Asthma	21.5	4.4	7.4	65.4	1.3	Few erythrocytes, loose mucus
Bronchial Asthma	96.1	0.8	0	1.8	1.3	-
Primary Ciliary Dyskinesia (PCD)	83	2.0	7.0	6.0	2.0	Erythrocytes
Bronchitis	96	3.0	3.0	0	1.0	Erythrocytes
Bronchiectasis	33	0	9	2	19	17% Undetermined Nuclei, 20% Epithelium, Mixed flora (moderate)
Pneumonia	81	2.0	3.0	0	14	-

CD68 serves as one of the markers of macrophages [43–46]. While eosinophils exhibit minimal CD68, their frequent co-occurrence with macrophages in inflammatory conditions means their combined presence can help predict the overall CD68-related inflammatory profile. Consequently, in bronchiectasis—a chronic respiratory disease characterized by permanently widened airways—the typically high macrophage percentage (in this case around 19%) strongly indicates significant CD68 staining, reflecting substantial inflammatory activity. The substantial macrophage population in pneumonia (14%) also suggests potential for CD68 positivity, although further investigation is needed to correlate staining intensity with inflammatory state. In eosinophilic asthma, despite a low macrophage percentage (1.3%), the remarkably high eosinophil count (65.4%) suggests sufficient CD68 expression might still be present, warranting further analysis to determine its contribution. Conversely, bronchial asthma, primary ciliary dyskinesia (PCD), and bronchitis, all exhibiting low macrophage percentages (1.3%, 2%, and 1%, respectively), and minimal eosinophils, are anticipated to show minimal CD68 staining. Immunohistochemical analysis using CD68 staining would validate these predictions, offering a quantitative assessment of macrophage and eosinophil contributions to CD68 expression.

3.3. Confocal Microscopy Analysis of Liposome Binding to BALF Cells

In order to further explore the interaction between our R6G-labelled DOPS/lecithin liposomes and BALF cells in the context of various respiratory disorders, we employed confocal laser scanning microscopy (CLSM) as a tool. BALF samples obtained from individuals with bronchitis (illustrated in the first two rows of Figure 3a) and bronchial asthma (third row) were carefully incubated with liposomes based on DOPS and lecithin. This approach provided invaluable insights into the

 doi:10.20944/preprints202508.0471.v1

morphological features of these critical immune and inflammatory cells, as well as the specific patterns of liposome attachment.

In the first row of the Figure 3a, we have BALF cells (at bronchitis) incubated with lecithin-based liposomes. Within this field, we can observe two distinct types of cells. On the left side, there is a typical phagocytic macrophage. These cells display a characteristic polymorphic morphology, characterized by an irregular shape and a single, distinct nucleus. On the right side, we observe a multinucleated macrophage, which has formed through the fusion of several cells. Its cytoplasm is densely filled with various vacuoles and phagosomes, indicating its active involvement in phagocytosis and the clearance of debris from the respiratory tract. This morphological feature aligns with the general representation of macrophages depicted in Figure 3b.

In row 2 of the Figure 3a, which involved BALF cells (at bronchitis) incubated with DOPS/lecithin liposomes, we observed a preponderance of M1-phenotype CD68+ macrophages. These macrophages typically exhibit a more rounded morphology with a more prominent cytoplasm compared to phagocytic macrophages. The strong expression of CD68, visualized through the binding of DOPS ligands, indicates an activated state, reflecting their increased secretory activity characteristic of the M1 phenotype. This is conceptually represented as "secretory type" macrophages in Figure 3b.

The third row in the experiment involving Bronchial asthma BALF cells incubated with DOPS/lecithin liposomes demonstrates the formation of foreign body giant cells (FBGCs), which are large, multinuclear cells that are a hallmark of chronic inflammation. These cells arise from the fusion of multiple macrophages in response to substances that are too large or insoluble for individual cells to clear, a process known as frustrated phagocytosis. Morphologically, FBGCs are characterized by their substantial size, multiple nuclei frequently clustered centrally, and expansive cytoplasm containing numerous phagosomes or entrapped material. Conceptually, as illustrated in Figure 3b, they represent the final stage of differentiation of mononuclear phagocytic cells and play a crucial role in the intricate inflammatory processes occurring within BALF. It is worth noting that minimal cell capture was observed when using plain lecithin, hence its exclusion from this study.

Figure 3b serves as a schematic representation that further aids in the classification of distinct cellular populations within BALF. It specifically depicts the characteristic morphologies of mature phagocytic and secretory macrophages, as well as epithelioid cells. This schematic serves as a complementary visual reference for CLSM images.

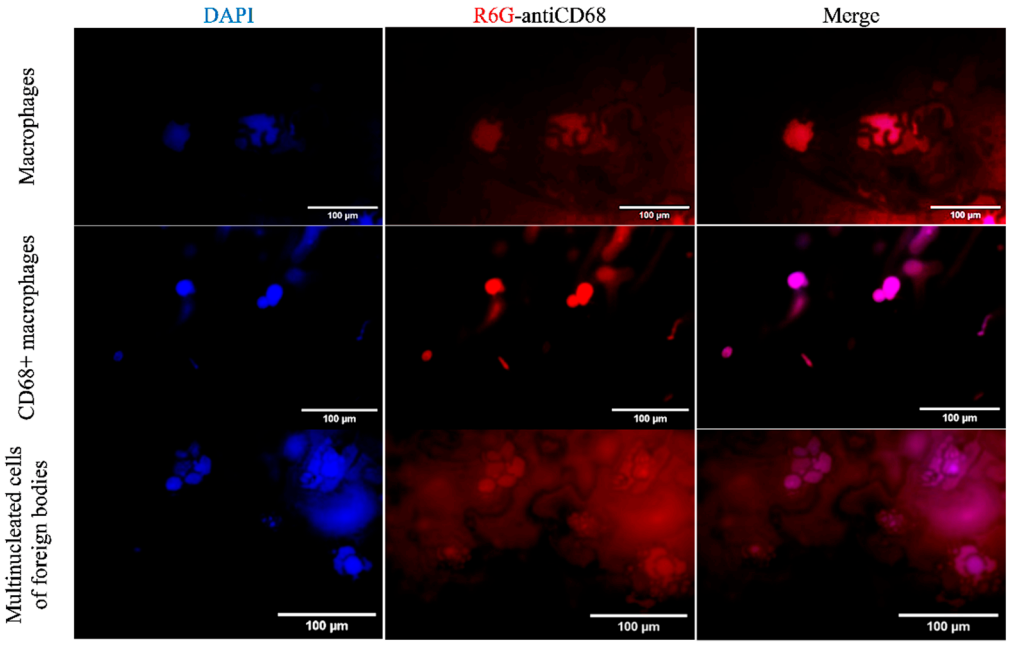

(a)

 doi:10.20944/preprints202508.0471.v1

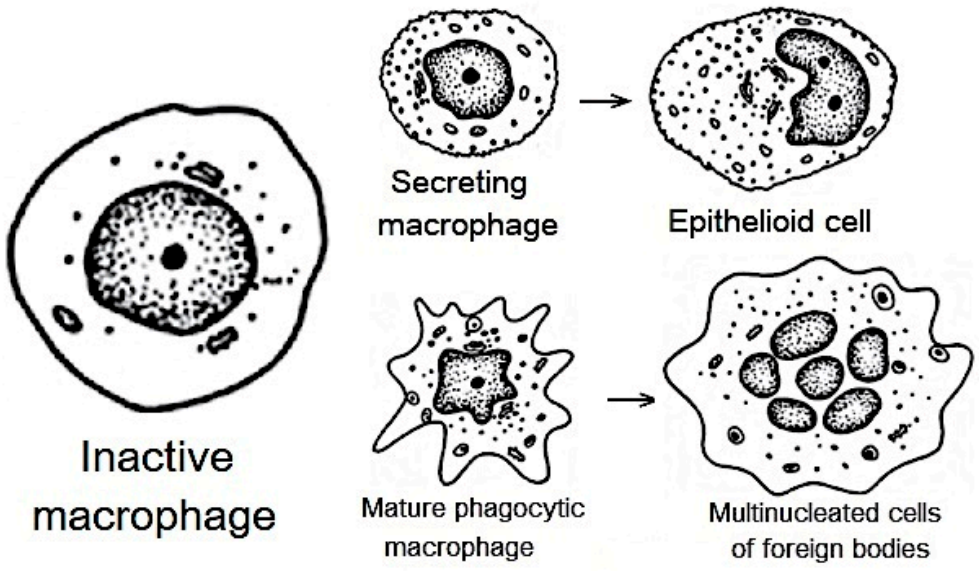

(b)

Figure 3. (a) CLSM images of macrophages in BALF from patients with Bronchitis (1st - 2nd rows) and Bronchial asthma (3rd row). PBS (0.01M, pH 7.4). T = 37 °C. Nuclei were stained with DAPI. DOPS/lecithin-based liposomes were labelled with R6G and used for CD68 receptors visualization. DAPI fluorescence was detected using following parameters: λexci,max = 340 nm, λemi = 410-500 nm. R6G fluorescence was detected using following parameters: λexci,max = 520 nm, λemi = 570-700 nm. (b) Schematic representation of macrophages, multinucleated cells. Adapted from [44].

To quantitatively assess the liposome binding, we analyzed the integral values of cell-associated fluorescence signals obtained from processing these CLSM images, as summarized in Table 3.

Table 3. Integral values of the cell-associated fluorescence signal obtained by processing CLSM images – Figure 3.

BALF cells	Signal intensity, a.u.	Background intensity, a.u	Signal/Background ratio	Colocalization of R6G(liposomes) with DAPI(nuclei)
Mature Macrophages	75±10	7±1	11±3	±
Secreting type macrophages	157±23	2±0.4	79±27	+
Multinuclear cells of foreign bodies	85±8	4±0.5	21±5	±

As is evident from Table 3, the CD68+ secreting type macrophages exhibited the highest signal intensity (157 a.u.) and, crucially, the most impressive Signal/Background ratio of 79. This significantly higher ratio, compared to other type of macrophages (11) and multinucleated cells (21), strongly indicates that our DOPS/lecithin liposomes preferentially bind to cells with elevated CD68 expression, confirming the specificity of our DOPS-based marker for mature, activated macrophages. While all three cell types showed detectable binding, the enhanced signal in CD68+ mature macrophages underscores the utility of our system in identifying and quantifying this specific, diagnostically relevant subpopulation.

 doi:10.20944/preprints202508.0471.v1

3.4. FTIR Spectroscopy Analysis of CD68 Status of BALF Immune Cells

3.4.1. Methodology and Confirmation of Liposome- BALF CD68+ Cells Binding Specificity

To investigate the molecular-scale interactions between our liposomes and immune cells, particularly CD68+ cells (macrophages) isolated from BALF, and gain insights into their binding dynamics, we utilized Fourier Transform Infrared (FTIR) spectroscopy. This powerful analytical technique provides detailed information about chemical structure, secondary structure changes, and conformational dynamics of biomolecules, allowing for real-time monitoring of subtle spectral alterations in liposomes upon interaction with target cells.

Figure 4a presents the time-resolved FTIR spectra of DOPS/lecithin-based liposomes (10/90 w/w) loaded with R6G, obtained upon incubation with CD68+ cells isolated from BALF samples of patients with bronchial asthma. Control FTIR spectra for pure lecithin-based and DOPS-based liposomes are provided in Figure S2. Our analysis primarily focuses on the Amide I region (1600-1700 cm–1), sensitive to protein secondary structures, and the ν(CH2) region (2800-3000 cm–1), which reflects the lipid acyl chain organization. Figure 4b further illustrates the kinetic changes in key FTIR spectral features (Amide I maximum position and intensity, ν(CH2,s) and ν(CH2,as) maximum positions), reflecting dynamic alterations upon liposome interaction with the cell surface.

The observed time-dependent changes in the FTIR spectra provide strong evidence for the interaction of DOPS-containing liposomes with CD68+ cells. The shift in the Amide I peak position, coupled with an increase in intensity, suggests conformational changes or altered microenvironment of cellular proteins upon liposome binding. The shifts observed in the ν(CH2,s) and ν(CH2,as) positions indicate reorganization of lipid acyl chains, likely involving both liposomal and cellular membrane lipids. These changes are consistent with mechanisms such as liposome adsorption, insertion, or fusion into the cell membrane. While further experiments are needed to definitively quantify selectivity, the observed spectral changes and their specific kinetic profiles are consistent with a significant interaction between DOPS-containing liposomes and BALF CD68+ cells, supporting the potential for targeted cellular interaction by our liposomal system.

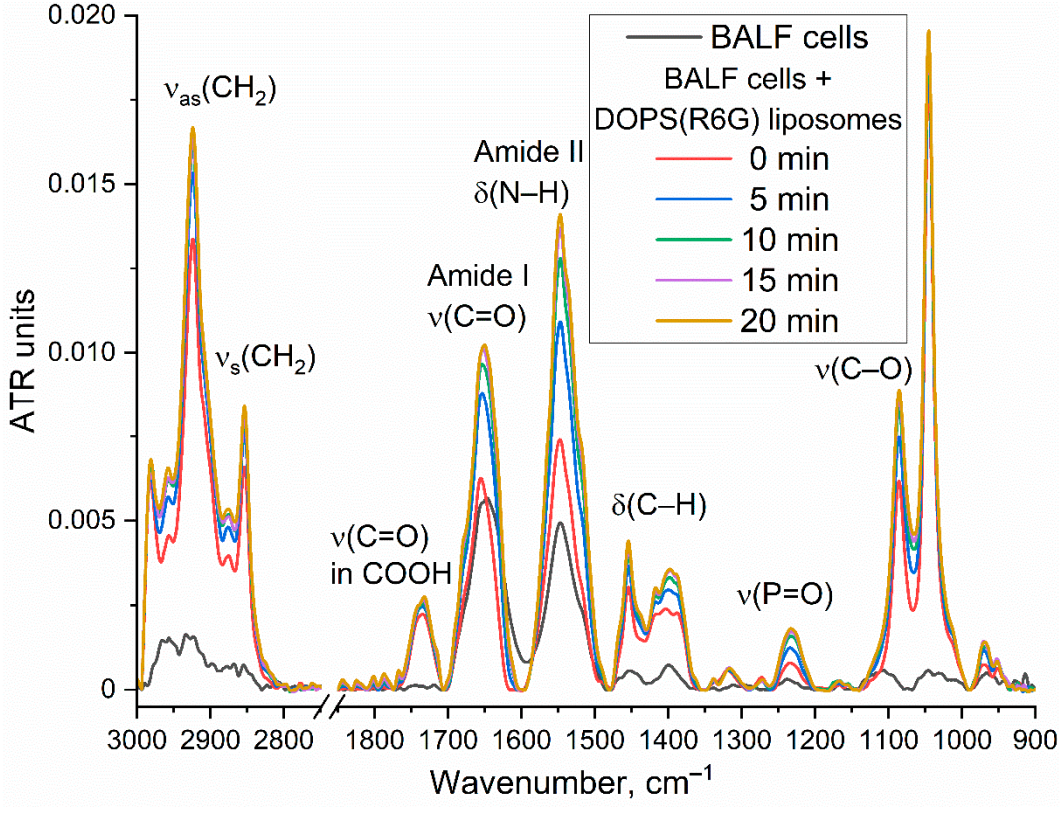

(a)

 doi:10.20944/preprints202508.0471.v1

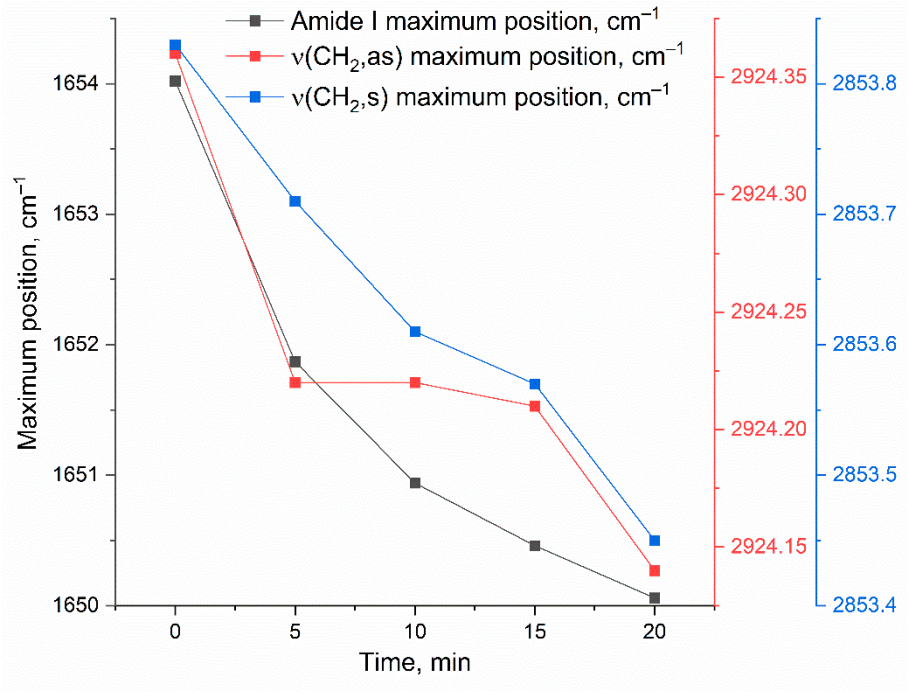

(b)

Figure 4. (a) FTIR spectra and (b) corresponding kinetic curves of FTIR peaks positions of DOPS/lecithin-based liposomes (10/90 w/w) loaded with R6G upon binding to eosinophils in BAL from patients with bronchial asthma. Without the addition of cellular components, there is essentially no alteration in the positions of lipid signals (<5% variation in signal upon binding to cells). PBS (0.01M, pH 7.4). T = 37 °C.

3.4.2. FTIR-Based Optimization of Liposome Composition for Differential Diagnosis of Respiratory Diseases

This section details the strategic use of FTIR spectroscopy to optimize liposome composition, specifically DOPS content, for enhanced differential diagnostic capability based on distinct cellular interactions in BALF from different patient disease states (e.g., Bronchiectasis vs. Bronchial Asthma). FTIR's ability to reveal subtle, disease-specific characteristics through quantitative differences in binding indices offers a novel method for identifying molecular signatures not always discernible via standard analyses.

To determine the optimal lipid film composition, particularly the DOPS mass content, for improved diagnostic differentiation across patient groups, we employed FTIR spectroscopy to monitor subtle alterations in cell-lipid interactions dependent on the disease state (Figure 5). Kinetic analyses focused on two analytically significant frequencies: the 1732 cm^{-1} (ν(C=O)) band, reflecting lipid headgroup hydration and conformation, and the 2923 cm^{-1} (ν(CH_2)) band, sensitive to hydrophobic core packing and fluidity. While both frequencies provided complementary information, the 2923 cm^{-1} peak was identified as particularly critical for optimizing DOPS concentration due to its direct correlation with membrane fluidity and its utility in characterizing robust binding dynamics (as exemplified in Figure 5d,f).

Figure 5g illustrates the binding efficiency as a function of DOPS mass content, revealing distinct optimal compositions tailored to specific patient conditions. For BALF samples from patients with Bronchiectasis (2% eosinophils and 19% macrophages), the maximal binding efficiency (39%) was observed at a 50% DOPS mass content. In contrast, for Bronchial Asthma samples (1.8% eosinophils and 1.3% macrophages), the binding efficiency is lower (35%) at 50% DOPS and continually increased with the concentration of DOPS phospholipid, reaching its maximum (55%) at 100% DOPS. The largest absolute difference in binding efficiency between these two patient groups was also observed at 100% DOPS mass content (32% for Bronchiectasis vs. 55% for Bronchial Asthma).

 doi:10.20944/preprints202508.0471.v1

Crucially, for optimal diagnostic discrimination between these disease states, particularly when elucidating macrophage interaction profiles, our analysis suggests that a DOPS mass content in the 25 % range offers superior analytical value. While 100% DOPS demonstrated the highest overall binding percentages, the lower concentration range provides for more stable liposomal particles and would enhance the selectivity of interaction with CD68+ macrophages, thus providing a more potent diagnostic signal for distinguishing between diseases.

Kinetic curves (Figures 5c-f) indicated that the most significant spectral changes occurred within the initial 5-10 minutes of interaction, subsequently reaching a plateau. This rapid stabilization suggests an optimal analysis time within 15-20 minutes for practical diagnostic applications.

In summary, the optimized FTIR spectroscopic parameters—focusing on 25% DOPS films, kinetic analysis up to 15-20 minutes, and primary monitoring of the 2923 cm^{-1} band—provide a refined methodology for sensitive and differential analysis of cellular interactions in BALF, paving the way for improved diagnostic tools.

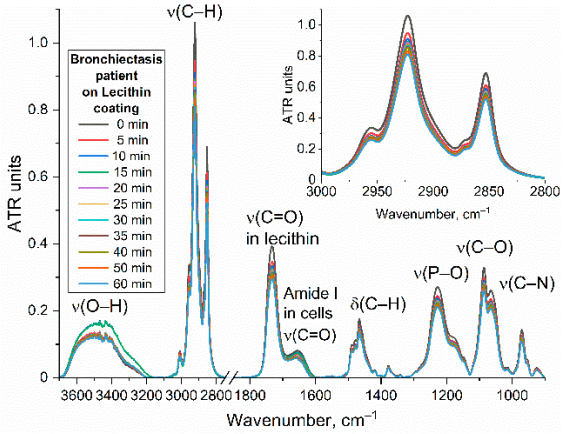

(a)

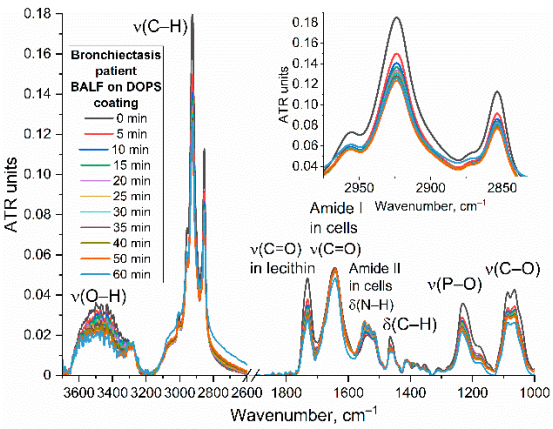

(b)

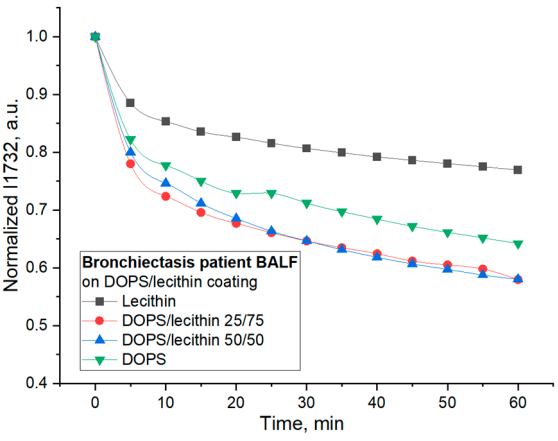

(c)

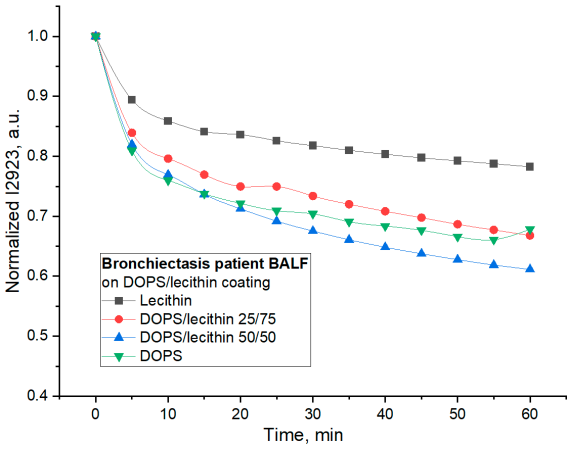

(d)

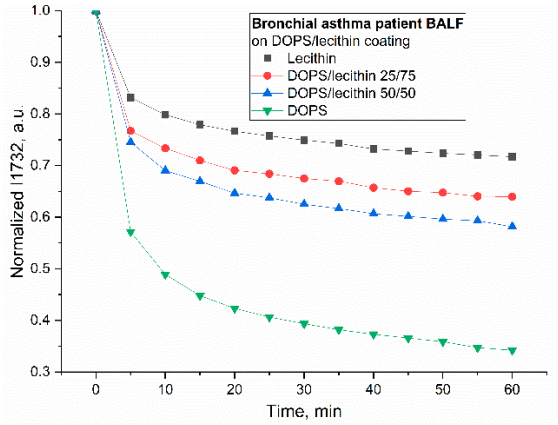

(e)

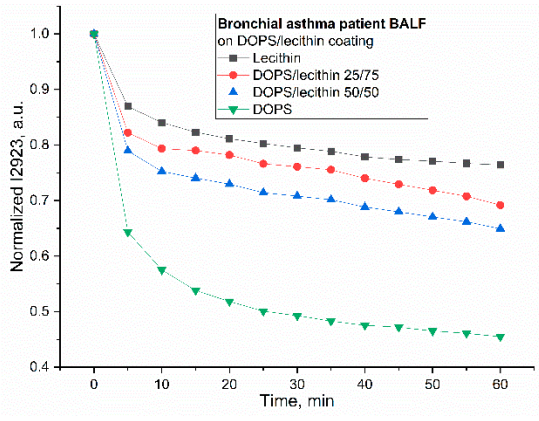

(f)

 doi:10.20944/preprints202508.0471.v1

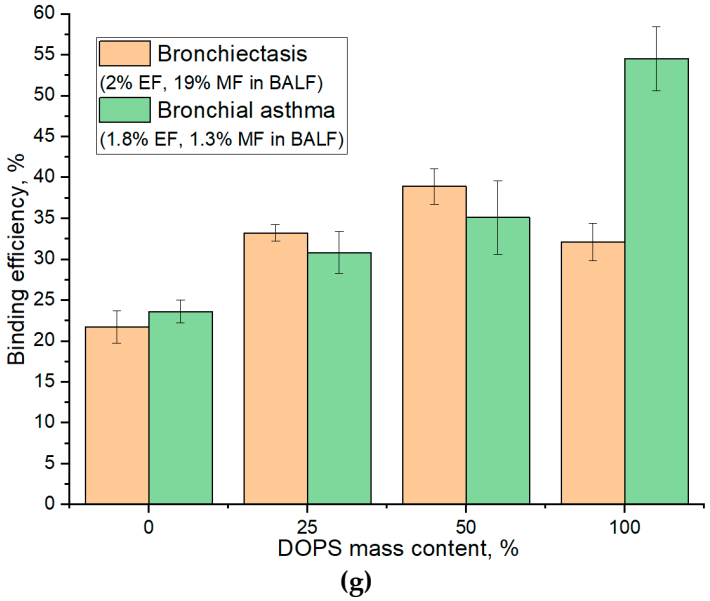

Figure 5. FTIR spectra of (a) a lecithin film and (b) DOPS film during interaction with cells from BALF samples from patient with Bronchiectasis. The corresponding kinetic curves of the peak intensity dependence at (c) 1732 cm^{-1} (ν(C=O)) and (d) 2923 cm^{-1} (ν(CH_2)) as a function of time for the BALF samples from patient with Bronchiectasis. The kinetic curves of the peak intensity dependence at (e) 1732 cm^{-1} (ν(C=O)) and (f) 2923 cm^{-1} (ν(CH_2)) as a function of time for the BALF samples from patient with asthma. (g) The indices of binding (based on ν(CH_2)) of the BALF samples with lecithin and DOPS traps. T = 37 °C.

3.4.3. PEGylated Stealth Liposomes for Defining CD68 Subtypes

A significant challenge in achieving high binding specificity in biosensing applications is the contribution of non-specific interactions, notably from common membrane components like lecithin, which can lead to considerable baseline binding and confound specific signal detection. To overcome this non-specific binding and enhance the diagnostic specificity of our assay for CD68+ populations, we employed PEGylated stealth liposomes incorporating a PEG-lipid (1-10 mass. %). This modification aims to create a steric barrier on the liposome surface, thereby reducing non-specific protein adsorption and cellular adhesion, ultimately improving the signal-to-noise ratio and thus the diagnostic utility of binding indices DOPS vs lecithin (e.g., aiming for robust differentiation beyond typical baseline values of 1.3-1.5 for bronchiectasis and ~2.5 for asthma).

Specifically, 1,2-Distearoyl-sn-glycero-3-phosphorylethanolamine polyethylene glycol (DSPE-PEG_{2000}) was incorporated into the lipid traps. Figure 6b presents FTIR spectra of a DOPS/lecithin (75/25 w/w) film interacting with BALF cells from bronchial asthma patients, with varying concentrations of incorporated DSPE-PEG_{2000}. The corresponding kinetic curves (Figure 6c) illustrate the effect of increasing DSPE-PEG_{2000} concentration on the binding kinetics.

In Bronchial Asthma samples, the binding index of liposomes with BALF cells initially decreased with the addition of 3% DSPE-PEG_{2000}, indicating an effective reduction in non-specific interactions. However, a subsequent increase in binding was observed at higher DSPE-PEG_{2000} concentrations (10-33%). This intriguing phenomenon suggests that excessively high PEGylation might lead to altered surface properties of liposomes or induce alternative non-specific interactions, potentially due to changes in the conformation of PEG chains or effects on membrane mechanics. In contrast, eosinophilic asthma exhibited a distinct and more straightforward trend: the binding index decreased monotonically with increasing DSPE-PEG_{2000} concentration. This consistent reduction demonstrates effective competition for binding sites and a lack of significant increase in non-specific binding even at higher PEG concentrations. This implies that in eosinophilic asthma, the interaction with the DOPS/lecithin film is predominantly specific to the target (CD68 receptors of immune cells), and PEGylation robustly masks non-specific interactions, leaving primarily the desired DOPS-mediated interaction. These results strongly suggest that the PEGylated liposome approach provides a valuable

 doi:10.20944/preprints202508.0471.v1

tool to differentiate the specific binding characteristics of cells in eosinophilic versus non-eosinophilic asthma, potentially reflecting underlying differences in membrane receptor expression or interaction mechanisms.

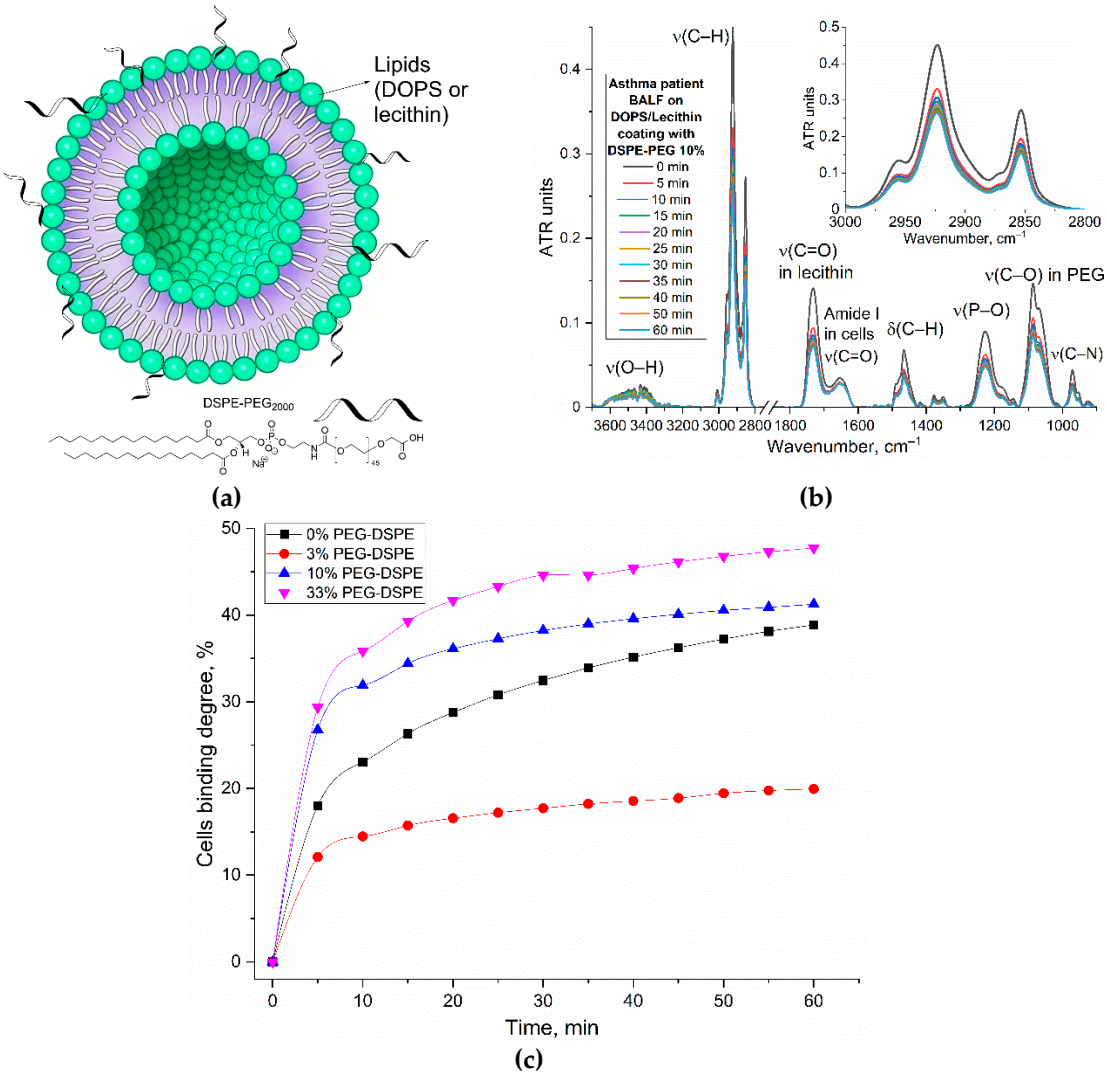

Figure 6. (a) A schematic representation of PEGylated liposomes**.** (b) FTIR spectra of DOPS/lecithin (75/25 w/w) film with addition of PEGylated lipid DSPE-PEG2000 during interaction with cells from BALF sample obtained from patients with bronchial asthma. (c) Corresponding kinetic curves from (b) for experiments with varying DSPE-PEG concentrations in BALF samples from bronchial asthma patients. T = 37 °C.

Here, we investigate the impact of varying DSPE-PEG content on the relative binding index of liposomes and, crucially, on the selectivity of their interaction with CD68, using the relative binding index data presented in Figure 7. The relative binding index demonstrates distinct trends across different liposome compositions.

 doi:10.20944/preprints202508.0471.v1

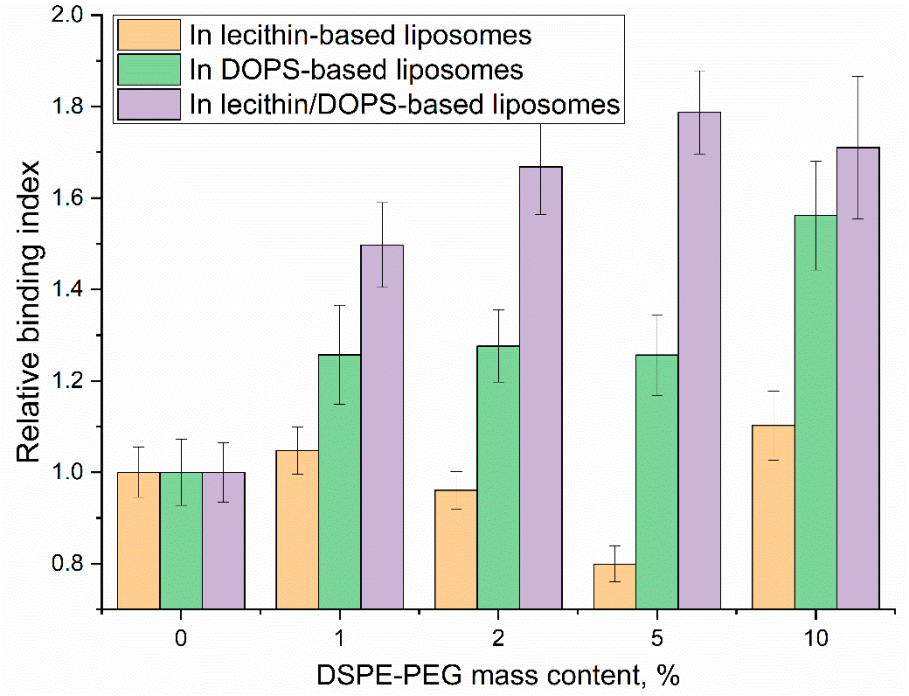

Figure 7. The binding indices of the BALF sample obtained from patients with bronchial asthma with traps: DOPS-based, lecithin-based and lecithin/DOPS (90/10 w/w)-based liposomes. Fluorometric detection using R6G. T = 37 °C.

The incorporation of DSPE-PEG significantly enhanced the specific binding performance of DOPS-containing liposomes. Both DOPS-only and lecithin/DOPS-based systems exhibited improvements in their specific binding indices. While DOPS-only showed peak binding at 10% DSPE-PEG (index 1.6), the most pronounced enhancement for lecithin/DOPS-based films was observed at 5% DSPE-PEG, achieving a specific binding index of 1.8. Crucially, at this optimal 5% DSPE-PEG concentration for the lecithin/DOPS formulation, the specific binding index (1.8) was substantially higher than that observed for DOPS-only system at the same concentration (index 1.3). This significant difference highlights the superior selectivity achieved with the lecithin/DOPS formulation at 5% PEG, indicating its enhanced ability to differentiate specific interactions. This improvement underscores that PEGylation, by creating a steric barrier, effectively mitigates non-specific interactions, thereby allowing the specific CD68-mediated binding to DOPS to become more prominent and efficient.

Mechanistically, PEGylation forms a hydrophilic "brush" on the liposome surface, which primarily functions by:

1. Reducing non-specific adhesion: Steric hindrance from PEG chains minimizes non-specific electrostatic or hydrophobic interactions, particularly those involving neutral lecithin components.
2. Optimizing specific ligand presentation: By suppressing non-specific binding, the relative contribution and effective presentation of the specific CD68-DOPS interaction are significantly amplified (potentially up to 3-fold), thus greatly increasing the signal-to-noise ratio for CD68-mediated recognition of anionic phospholipids.

The observed optimal selectivity at 5% DSPE-PEG suggests a critical balance: the PEG corona is sufficiently dense to mask non-specific binding sites while preserving optimal accessibility of DOPS for specific CD68 recognition. Higher PEG concentrations (e.g., 10-33%) may introduce some liposomes destabilization, excessive steric hindrance, potentially slightly impeding the specific ligand-receptor interaction itself, leading to a minor reduction in selectivity.

These findings conclusively demonstrate that optimized PEGylation (5% DSPE-PEG) dramatically enhances the selectivity of CD68-mediated binding to DOPS-containing liposomes. This

 doi:10.20944/preprints202508.0471.v1

not only confirms PEG's role in improving liposomal stability but, more critically, refines the specificity of receptor-mediated targeting, offering a powerful tool for developing precise diagnostic agents or therapeutic carriers for CD68-expressing cells like macrophages.

3.5. Fluorimetric Detection of CD68 Receptors on Macrophages and Eosinophils in Order to Differentiate Diagnoses

To complement and further validate our findings from FTIR and CLSM analyses, and to confirm the enhanced selectivity observed with PEG-DOPS liposomes, we developed a fluorimetric method for different diagnosis based on CD68 receptor profiling. This assay specifically quantifies the interaction of BALF-derived CD68-positive cells with DOPS/lecithin-based liposomes. The liposomes were designed to encapsulate rhodamine 6G (R6G) as a fluorescent reporter. Figure 8 displays the kinetic curves of R6G fluorescence signal over 60 minutes following incubation with BALF cells from patients across various pulmonary diagnoses. Crucially, the contribution of non-specific binding from lecithin-based liposomes was rigorously accounted for and subtracted, ensuring that the measured fluorescence signal exclusively reflected specific CD68-mediated interactions with DOPS.

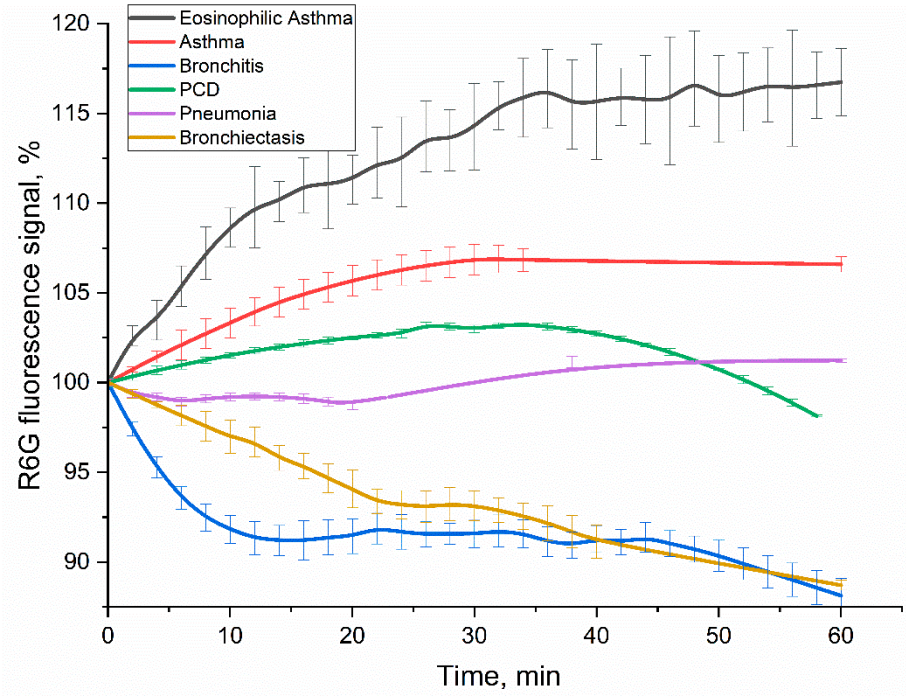

Figure 8. Kinetic curves of R6G fluorescence in DOPS/lecithin-based liposomes upon binding to cells in BALF from patients. A standard analysis in accordance with the scheme — Figure 1. The contribution to the binding of lecithin-based liposomes is taken into account as background. The number of cells was 5×10^5 per well, the concentration of lipids was 0.1 mg/mL, and the concentration of R6G was 1 μg/mL. PBS (0.01M, pH 7.4). T = 37 °C.

It is well-established that R6G fluorescence can be significantly quenched upon cellular uptake or interaction with intracellular environments. Indeed, our previous control experiments involving direct incubation of rhodamine 6G with cell lines such as A549 and K562 consistently demonstrated such quenching, evident as a reduction in fluorescence intensity [47]. This phenomenon provides a plausible explanation for the observed decrease in rhodamine fluorescence in our current system upon interaction with BALF cells.

The kinetic profiles of R6G fluorescence signal change varied significantly across different diagnoses (Figure 8), providing **distinct patterns as potential diagnostic signatures**. In order to interpret the kinetic profiles, it is necessary to delineate the stages of the process involving

 doi:10.20944/preprints202508.0471.v1

rhodamine. Liposomal R6G initially binds to cells, and either fusion or receptor-mediated endocytosis takes place; or phagocytosis, which is a response to large particles such as liposomes. These processes ultimately determine the variation in the fluorescent signal. Binding to the receptor within the hydrophobic pocket appears to amplify the signal emitted by R6G fluorescence. Conversely, fusion with the cellular membrane and the subsequent formation of endosomes lead to a reduction in fluorescence. Subsequently, once rhodamine enters lysosomes after approximately 20 minutes, it undergoes a process of digestion in an acidic environment. This indicates that regions with more intense fluorescence correspond to areas with a higher concentration of CD68+ receptors. Conversely, regions with a negative slope suggest primarily involve non-specific liposome fusion without receptor involvement.

1. **Positive signal response.** In case of **eosinophilic asthma** BALF samples (*with M2 macrophage phenotype*) showed the most pronounced and sustained R6G fluorescence increase (over 16% within 1h). This increased fluorescence signal correlates with their exceptionally high BALF eosinophil counts (65.4%), accompanied with intensive CD68 receptor activity and specific liposome binding and internalization by the cells. Other type of BALF (Bronchial Asthma: 1.8% eosinophils, 1.3% macrophages; PCD: 6.0% eosinophils, 2.0% macrophages) also exhibited a fluorescence increase, consistent with active interaction of DOPS/lecithin-based liposomes with CD68+ cells populations.
2. **Negative signal response.** In contrast, **bronchitis** (1.0% macrophages, 96% neutrophils) and **bronchiectasis** (19% macrophages, 33% neutrophils) patients' BALFs showed a marked and persistent R6G fluorescence decline (approx. 11% reduction within 1h). This remarkable quenching phenomenon, observed in the presence of macrophages, suggests the existence of an alternative interaction mechanism. It is possible that this mechanism involves the active phagocytosis of R6G-liposomes or their fusion with the biomembrane, resulting in the loss of fluorescence. Alternatively, it may be associated with a distinct phenotype of macrophages, compared to pro-inflammatory M1-type.
3. Minimal signal response. The BALF sample from a patient with **pneumonia**, which contained 14% macrophages and 81% neutrophils, exhibited minor alterations in R6G fluorescence. These findings suggest a delicate equilibrium between CD68-mediated interactions and non-specific interactions, such as phagocytosis of large particles and fusion, which leads to the quenching of rhodamine. This suggests a more intricate or transient cellular response, rather than a clear net uptake or quenching, indicating a mixed M0/M1/M2 phenotype.

The divergent kinetic profiles of R6G fluorescence observed across different disease states underscore the potential of this fluorimetric assay as a tool for differential diagnosis. The unique "kinetic pattern" reflecting the interaction of BALF cells with DOPS-containing liposomes provide valuable insights into the functional state and receptor activity of macrophages in various pulmonary pathologies. The clear distinction between positive (asthma, PCD) and negative (bronchitis, bronchiectasis) fluorescence changes, combined with the minimal response in pneumonia, suggests that this methodology could significantly aid in the sub-classification of respiratory diseases.

3.6. Diagnostic Performance Evaluation: Liposome Binding Kinetics and Correlation with Clinical Parameters

Based on the kinetic profiles of liposome binding to eosinophils in BALF, we aimed to evaluate the diagnostic performance of our approach. We focused on quantifying the initial binding rate (Initial binding index, %/min), reflecting the early interaction kinetics, and the effective binding index over a 1-h period (Effective binding index for 1 h, %), representing the overall interaction outcome (Figure 9). These indices represent a simplified yet powerful "fingerprint" for patient diagnosis based on the distinct cellular interactions with DOPS/lecithin-based liposomes loaded with R6G. As before, background fluorescence from lecithin-based liposomes was subtracted to isolate specific CD68-mediated interactions.

 doi:10.20944/preprints202508.0471.v1

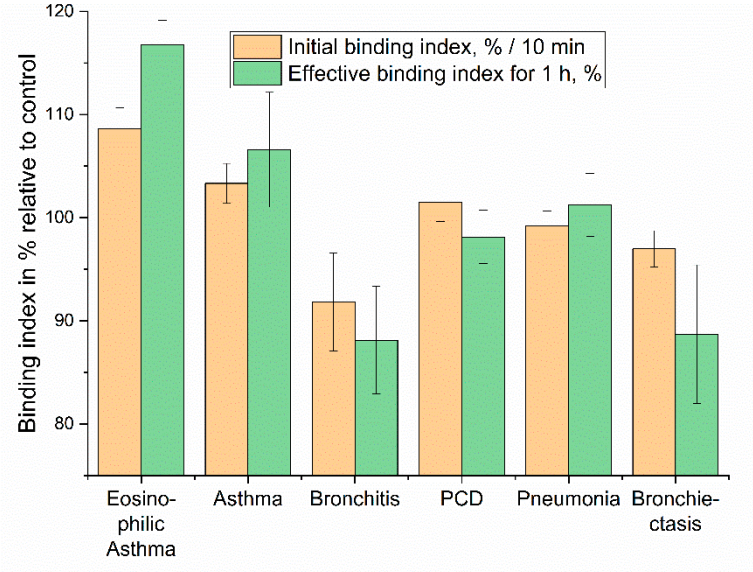

Figure 9. Examples of fingerprint fluorescent typing (diagnosis) of patients based on their BALF samples in the context of binding with DOPS/lecithin-based liposomes loaded with R6G. The contribution to the binding of lecithin-based liposomes is taken into account as background. The number of cells was 5×10^5 per well, the concentration of lipids was 0.1 mg/mL, and the concentration of R6G was 1 μg/mL. PBS (0.01M, pH 7.4). T = 37 °C.

The "Initial binding index" captures the early phase of the cellular interaction, specifically reflecting the change in R6G fluorescence at the 10-minute mark. This metric is indicative of the rapid cellular recognition and initial binding kinetics. The "Effective binding index for 1 hour" represents the cumulative fluorescence change, providing insight into the sustained cellular processing of the liposomes and the eventual fate of the encapsulated R6G. This two-parameter approach enables the differentiation of conditions that might otherwise present similar clinical symptoms, highlighting the potential for this assay to refine diagnostic precision in respiratory medicine.

3.7. Comparative Analysis of Macrophage Receptor Activity in Pulmonary Diseases

To quantitatively compare liposome-cell interactions across different analytical platforms, binding indices were derived from both fluorescence kinetic data (Figure 8 and 9) and endpoint FTIR spectroscopy (Figure 5 and 6). Fluorescence data yielded an **Initial Rate Index** (calculated from the first 10 minutes, %/min) and an **Effective Binding Index** (% change at 60 min). FTIR data provided a **DOPS-Specific Binding Index** (calculated as the percentage point increase in binding efficiency between 0% and 100% DOPS liposomes).

Both methodologies demonstrate concordant trends, highlighting a higher **Effective Binding Index** and thus, significantly stronger ligand-receptor interaction in asthma phenotypes. FTIR analysis reveals a nearly 3-fold greater DOPS-specific binding for bronchial asthma compared to bronchiectasis (+30.5% vs. +10.5%). This aligns with fluorescence data, where eosinophilic and bronchial asthma show positive indices, reflecting high surface binding or accessibility. In contrast, bronchitis and bronchiectasis exhibit negative indices, indicating significant fluorescence quenching likely due to rapid internalization and lysosomal processing.

These insights into the activity of the pan-macrophage marker CD68 complement previous findings on the M2-phenotype marker CD206 [9] and phagocytic activity [10], allowing for a more nuanced characterization of the macrophage landscape (Table 4):

- **Bronchiectasis:** This condition is characterized by chronic infection and a resulting pro-inflammatory state dominated by M1 macrophages. The assay accurately reflects this pathology, yielding a signature of weak binding to the M2-specific CD206 marker coupled with a strong

 doi:10.20944/preprints202508.0471.v1

interaction with the CD68-DOPS probe. Critically, this strong interaction manifests as significant fluorescence quenching. M1 macrophages are "classically activated" phagocytes, primed to engulf and destroy pathogens and cellular debris. The observed quenching strongly suggests that the fluorescent DOPS -liposomes, which mimic apoptotic bodies, are not only binding to the M1 cells but are being rapidly internalized and trafficked into the acidic, degradative environment of the phagolysosome. This process denatures or degrades the fluorophore, leading to a measurable decrease in signal. Therefore, the quenching serves as a direct proxy for robust, M1-driven phagocytic activity.

- **Asthma:** In asthma, our assay revealed a high CD206 marker signal, consistent with the literature's description of a dominant M2 anti-inflammatory/remodeling macrophage phenotype. This was coupled with a high CD68-DOPS probe signal, suggesting a substantial M2 macrophage population or high surface receptor accessibility contributing to the observed immune profile.
- **Bronchitis:** For bronchitis, our data indicated a high CD206 marker signal with fluorescence quenching, aligning with a literature-supported M1-phenotype and mixed macrophage presence. The observed high CD68-DOPS probe signal, particularly with quenching, infers an active pro-inflammatory state, potentially with significant phagocytic activity characteristic of M1 macrophages or a mixed inflammatory response.
- **Pneumonia:** Acute bacterial pneumonia presents a highly dynamic and heterogeneous immune landscape, reflecting the complex and rapidly evolving phases of infection, acute inflammation, and subsequent resolution. The macrophage population is a mixture of resident cells, newly recruited monocytes (M0), pro-inflammatory M1 cells fighting the infection, and emerging M2 cells mediating repair. The assay successfully captures this complexity, generating a signature of intermediate CD206 binding and a minimal, fluctuating signal from the CD68 probe. This fingerprint is consistent with a mixed, transitional population of macrophages in various states of activation, phagocytosis, and functional polarization.

Table 4. Disease-specific immunophenotypes.

Disease	Dominant Macrophage Phenotype (Literature)	CD206 Marker Signal (Our assay [9])	CD68-DOPS Probe Signal (This paper)	Inferred Functional State & Interpretation
Bronchiectasis	M1 (Pro-inflammatory) [48]	Low	High (with fluorescence quenching)	High phagocytic activity; active pro-inflammatory state
Asthma	M2 (Anti-inflammatory) [49]	High	High	High M2 population and/or high surface receptor accessibility
Bronchitis	M1-phenotype and mixed [49]	Intermediate	High (with fluorescence quenching)	Pro-inflammatory state
Pneumonia	Mixed M0/M1/M2 (Dynamic) [50]	Intermediate	Minimal / Fluctuating	Heterogeneous population reflecting acute

 doi:10.20944/preprints202508.0471.v1

				inflammation and resolution phases

In conclusion, this multi-marker comparison, leveraging quantitative indices from both CD68 and CD206 interactions, provides a more comprehensive understanding of the macrophage activation spectrum in BALF. The functional activity of CD68 (probing general engagement and uptake) combined with the phenotypic specificity of CD206 (profiling M2 polarization) offers enhanced diagnostic precision by characterizing not just the presence but also the functional state of key immune cell populations.

4. Conclusions

In this study, we investigated the analytical significance of CD68+ cells for the differential diagnosis of respiratory disorders, culminating in the development of a novel liposome-based assay utilizing the dioleoylphosphatidylserine (DOPS) marker as a sophisticated alternative to traditional antibody-based methods. Recognizing the profound phenotypic heterogeneity and functional plasticity of macrophages, our goal was to engineer a precise diagnostic tool capable of overcoming the limitations of conventional approaches by specifically targeting these dynamic immune cells. Our strategy is based on a meticulously designed analytical platform where DOPS acts as a specific, high-affinity ligand for CD68, a design rigorously validated by *in silico* modeling (achieving a pK_d of 7.2 for DOPS versus 5.6 for lecithin).

We meticulously optimized the liposome formulation, demonstrating that increasing DOPS content (optimal at approximately 25%) significantly enhanced target binding. Crucially, the engineering of PEGylated "stealth" liposomes (optimal at 5% DSPE-PEG) boosted specificity up to threefold by effectively shielding against non-specific interactions. The robust and specific interaction of this innovative probe with target cells was thoroughly validated across a suite of advanced methods, including fluorescence microscopy, Confocal Laser Scanning Microscopy (CLSM), and Fourier-transformed infrared (FTIR) spectroscopy.

Furthermore, we developed a versatile fluorimetric assay that generates unique "binding fingerprints" of BALF cells. These fingerprints offer deep insight into the CD68+ cell subpopulations driving distinct respiratory diseases, particularly when seamlessly integrated with our previous findings on the M2-specific CD206 marker. Our comprehensive analysis revealed distinct cellular immunophenotypes that effectively differentiate respiratory disease profiles. **Bronchiectasis** was clearly characterized by a predominant M1 macrophage phenotype, evidenced by weak CD206 binding coupled with a strong CD68-DOPS probe interaction that manifested as significant fluorescence quenching. This profile likely reflects robust M1-driven phagocytic activity and a pro-inflammatory state. **Asthma** demonstrated a pronounced M2 macrophage phenotype with elevated CD206 binding and a significantly increased CD68-DOPS fluorescence signal, potentially reflecting high CD68 surface accessibility or a larger overall macrophage population within this M2-rich environment. In contrast, **Bronchitis**, while also showing elevated CD206 binding, displayed a distinct CD68-DOPS binding profile. This suggests a notable M1 contribution alongside the M2 phenotype. Such nuanced differences are vital, potentially informing treatment strategies by helping to distinguish between conditions requiring standard antibiotic/mucolytic therapy and those with a higher risk of complications like bronchiectasis that might contraindicate specific treatments. **Pneumonia**, presented a mixed M0/M1/M2 macrophage binding profile, reflected in intermediate CD206 binding and a minimal, fluctuating CD68 signal consistent with the acute phases of infection.

In conclusion, this integrated multi-marker strategy, leveraging both the pan-macrophage CD68 probe and the M2-specific CD206 marker, provides a far more comprehensive and nuanced assessment of the immune profile in BALF than single-marker analysis. This approach paves the way for more precise and effective differential diagnoses in respiratory medicine and offers improved guidance for targeted therapeutic interventions.

 doi:10.20944/preprints202508.0471.v1

Supplementary Materials: The following supporting information can be downloaded at the website of this paper posted on Preprints.org. Figure S1. The structural basis of the specificity of phospholipid binding to the human CD68 receptor. Figure S2. FTIR spectra of lecithin-based and DOPS-based liposomes. PBS (0.01M, pH 7.4). T = 37 °C.

Author Contributions: Conceptualization, E.V.K., I.D.Z. and D.Y.O.; methodology, I.D.Z., S.A.G., A.A.E., N.I.K., D.Y.O. and E.V.K.; formal analysis, I.D.Z. and A.A.E.; investigation, I.D.Z., A.A.E., S.A.G. and E.V.K.; data curation, I.D.Z. and A.A.E.; writing—original draft preparation, I.D.Z.; writing—review and editing, E.V.K.; project supervision, E.V.K.; funding acquisition, E.V.K. All authors have read and agreed to the published version of the manuscript.

Funding: This research was funded by the Russian Science Foundation, grant number 24-25-00104.

Institutional Review Board Statement: Cell lines were obtained from Lomonosov Moscow State University Depository of Live Systems Collection (Moscow, Russia).

Informed Consent Statement: BALF samples were collected from the Morozovskaya Children's City Clinical Hospital with the patients' consent, ensuring strict adherence to ethical guidelines.

Data Availability Statement: The data presented in this study are available in the main text and in Supplementary Materials.

Acknowledgments: This work was performed using the following equipment from the program for the development of Moscow State University: the MICRAN-3 FTIR microscope, Jasco J-815 CD spectrometer, NTEGRA II AFM microscope, Olympus FluoView FV1000 confocal laser scanning microscope and Olympus IX81 motorized inverted microscope.

Conflicts of Interest: The authors declare no conflicts of interest.

Abbreviations

The following abbreviations are used in this manuscript:

BAL	Bronchoalveolar lavage
BALF	Bronchoalveolar lavage fluid
CLSM	Confocal laser scanning microscopy
CPR	C-reactive protein
DAPI	4′,6-diamidino-2-phenylindole
DOPS	Dioleoyl phosphatidylserine
FTIR	Fourier-transformed infrared spectroscopy

References

1. Tan, Q.; He, L.; Meng, X.; Wang, W.; Pan, H.; Yin, W.; Zhu, T.; Huang, X.; Shan, H. Macrophage Biomimetic Nanocarriers for Anti-Inflammation and Targeted Antiviral Treatment in COVID-19. *J. Nanobiotechnology* **2021**, *19*, 1–16, doi:10.1186/s12951-021-00926-0.
2. Tashkin, D.P.; Wechsler, M.E. Role of Eosinophils in Airway Inflammation of Chronic Obstructive Pulmonary Disease. *Int. J. COPD* **2018**, *13*, 335–349, doi:10.2147/COPD.S152291.
3. Charhouf, I.; Bennamara, A.; Abdelmjid, A.; Berrada, M. Characterization of a Dialdehyde Chitosan Generated by Periodate Oxidation International Journal of Sciences : Basic and Applied Research Characterization of a Dialdehyde Chitosan Generated by Periodate Oxidation. **2014**.
4. d'Alessandro, M.; Carleo, A.; Cameli, P.; Bergantini, L.; Perrone, A.; Vietri, L.; Lanzarone, N.; Vagaggini, C.; Sestini, P.; Bargagli, E. BAL Biomarkers' Panel for Differential Diagnosis of Interstitial Lung Diseases. *Clin. Exp. Med.* **2020**, *20*, 207–216, doi:10.1007/s10238-020-00608-5.
5. Qiaozhen, H.; Jifei, Z.; Lingrong, H.; Qiuming, Y.; Hongjuan, Y.; Qiaozhen, H. Clinical Significance of Detection of Mononuclear Phagocyte Subsets in Blood and Bronchoalveolar Lavage Fluid (BALF) in Pulmonary Sarcoidosis. *Cell. Mol. Biol.* **2021**, *67*, 109–116, doi:10.14715/CMB/2021.67.5.15.

 doi:10.20944/preprints202508.0471.v1

6. Gao, C.A.; Cuttica, M.J.; Malsin, E.S.; Argento, A.C.; Wunderink, R.G.; Smith, S.B. Comparing Nasopharyngeal and BAL SARS-CoV-2 Assays in Respiratory Failure. *Am. J. Respir. Crit. Care Med.* **2021**, *203*, 127–129, doi:10.1164/rccm.202008-3137LE.
7. Rai, R.K.; Azim, A.; Sinha, N.; Sahoo, J.N.; Singh, C.; Ahmed, A.; Saigal, S.; Baronia, A.K.; Gupta, D.; Gurjar, M.; et al. Metabolic Profiling in Human Lung Injuries by High-Resolution Nuclear Magnetic Resonance Spectroscopy of Bronchoalveolar Lavage Fluid (BALF). *Metabolomics* **2013**, *9*, 667–676, doi:10.1007/s11306-012-0472-y.
8. Zlotnikov, I.D.; Kudryashova, E. V. Biomimetic System Based on Reconstituted Macrophage Membranes for Analyzing and Selection of Higher-Affinity Ligands Specific to Mannose Receptor to Develop the Macrophage-Focused Medicines. *Biomedicines* **2023**, *11*, doi:10.3390/biomedicines11102769.
9. Zlotnikov, I.D.; Kudryashova, E. V. Polymeric Infrared and Fluorescent Probes to Assess Macrophage Diversity in Bronchoalveolar Lavage Fluid of Asthma and Other Pulmonary Disease Patients. *Polymers (Basel).* **2024**, *16*, 3427, doi:10.3390/polym16233427.
10. Zlotnikov, I.D.; Ezhov, A.A.; Kolganova, N.I.; Ovsyannikov, D.Y.; Belogurova, N.G.; Kudryashova, E. V. Optical Methods for Determining the Phagocytic Activity Profile of CD206-Positive Macrophages Extracted from Bronchoalveolar Lavage by Specific Mannosylated Polymeric Ligands. *Polymers (Basel).* **2025**, *17*, doi:10.3390/polym17010065.
11. Bafadhel, M. The Eosinophil in COPD : Just Another Biomarker ? 1–19.
12. Hiles, S.A.; Gibson, P.G.; McDonald, V.M. Disease Burden of Eosinophilic Airway Disease: Comparing Severe Asthma, COPD and Asthma–COPD Overlap. *Respirology* **2021**, *26*, 52–61, doi:10.1111/resp.13841.
13. George, L.; Brightling, C.E. Eosinophilic Airway Inflammation: Role in Asthma and Chronic Obstructive Pulmonary Disease. *Ther. Adv. Chronic Dis.* **2016**, *7*, 34–51, doi:10.1177/2040622315609251.
14. Kostikas, K.; Brindicci, C.; Patalano, F. Blood Eosinophils as Biomarkers to Drive Treatment Choices in Asthma and COPD. *Curr. Drug Targets* **2018**, *19*, 1882–1896, doi:10.2174/1389450119666180212120012.
15. Gut, G.; Armoni Domany, K.; Sadot, E.; Soferman, R.; Fireman, E.; Sivan, Y. Eosinophil Cell Count in Bronchoalveolar Lavage Fluid in Early Childhood Wheezing: Is It Predictive of Future Asthma? *J. Asthma* **2020**, *57*, 366–372, doi:10.1080/02770903.2019.1579829.
16. Sohn, J.W. Acute Eosinophilic Pneumonia. *Tuberc. Respir. Dis. (Seoul).* **2013**, *74*, 51–55, doi:10.4046/trd.2013.74.2.51.
17. Janz, D.R.; O'Neal, H.R.; Ely, E.W. Acute Eosinophilic Pneumonia: A Case Report and Review of the Literature. *Crit. Care Med.* **2009**, *37*, 1470–1474, doi:10.1097/CCM.0b013e31819cc502.
18. Philit, F.; Etienne-Mastroïanni, B.; Parrot, A.; Guérin, C.; Robert, D.; Cordier, J.F. Idiopathic Acute Eosinophilic Pneumonia: A Study of 22 Patients. *Am. J. Respir. Crit. Care Med.* **2002**, *166*, 1235–1239, doi:10.1164/rccm.2112056.
19. Wechsler, M.E.; Munitz, A.; Ackerman, S.J.; Drake, M.G.; Jackson, D.J.; Wardlaw, A.J.; Dougan, S.K.; Berdnikovs, S.; Schleich, F.; Matucci, A.; et al. Eosinophils in Health and Disease: A State-of-the-Art Review. *Mayo Clin. Proc.* **2021**, *96*, 2694–2707, doi:10.1016/j.mayocp.2021.04.025.
20. Rosenberg, H.F.; Dyer, K.D.; Foster, P.S. Eosinophils: Changing Perspectives in Health and Disease. *Nat. Rev. Immunol.* **2013**, *13*, 9–22, doi:10.1038/nri3341.
21. Todd, J.L.; Weber, J.M.; Kelly, F.L.; Neely, M.L.; Mulder, H.; Frankel, C.W.; Nagler, A.; McCrae, C.; Newbold, P.; Kreindler, J.; et al. BAL Fluid Eosinophilia Associates With Chronic Lung Allograft Dysfunction Risk: A Multicenter Study. *Chest* **2023**, *164*, 670–681, doi:10.1016/j.chest.2023.03.033.
22. Nelson, R.K.; Bush, A.; Stokes, J.; Nair, P.; Akuthota, P. Eosinophilic Asthma. *J. Allergy Clin. Immunol. Pract.* **2020**, *8*, 465–473, doi:10.1016/j.jaip.2019.11.024.
23. Bakakos, A.; Loukides, S.; Bakakos, P. Severe Eosinophilic Asthma. *J. Clin. Med.* **2019**, *8*, doi:10.3390/jcm8091375.
24. Mukae, H.; Kadota, J.I.; Kohno, S.; Matsukura, S.; Hara, K. Increase of Activated T-Cells in BAL Fluid of Japanese Patients with Bronchiolitis Obliterans Organizing Pneumonia and Chronic Eosinophilic Pneumonia. *Chest* **1995**, *108*, 123–128, doi:10.1378/chest.108.1.123.

 doi:10.20944/preprints202508.0471.v1

25. Matsuse, H.; Shimoda, T.; Fukushima, C.; Matsvo, N.; Sakai, H.; Takao, A.; Asai, S.; Kohno, S. Diagnostic Problems in Chronic Eosinophilic Pneumonia. *J. Int. Med. Res.* **1997**, *25*, 196–201, doi:10.1177/030006059702500404.
26. Alam, M.; Burki, N.K. Chronic Eosinophilic Pneumonia: A Review. *South. Med. J.* **2007**, *100*, 49–53, doi:10.1097/01.smj.0000242863.17778.1d.
27. Greenberger, P.A.; Smith, L.J.; Hsu, C.C.S.; Roberts, M.; Liotta, J.L. Analysis of Bronchoalveolar Lavage in Allergic Bronchopulmonary Aspergillosis: Divergent Responses of Antigen-Specific Antibodies and Total IgE. *J. Allergy Clin. Immunol.* **1988**, *82*, 164–170, doi:10.1016/0091-6749(88)90995-5.
28. Greenberger, P.A. Allergic Bronchopulmonary Aspergillosis. *J. Allergy Clin. Immunol.* **2002**, *110*, 685–692, doi:10.1067/mai.2002.130179.
29. Agarwal, R.; Sehgal, I.S.; Dhooria, S.; Muthu, V.; Prasad, K.T.; Bal, A.; Aggarwal, A.N.; Chakrabarti, A. Allergic Bronchopulmonary Aspergillosis. *Indian J. Med. Res.* **2020**, *151*, 529–549, doi:10.4103/ijmr.IJMR_1187_19.
30. Emmi, G.; Bettiol, A.; Gelain, E.; Bajema, I.M.; Berti, A.; Burns, S.; Cid, M.C.; Cohen Tervaert, J.W.; Cottin, V.; Durante, E.; et al. Evidence-Based Guideline for the Diagnosis and Management of Eosinophilic Granulomatosis with Polyangiitis. *Nat. Rev. Rheumatol.* **2023**, *19*, 378–393, doi:10.1038/s41584-023-00958-w.
31. Vaglio, A.; Buzio, C.; Zwerina, J. Eosinophilic Granulomatosis with Polyangiitis (Churg-Strauss): State of the Art. *Allergy Eur. J. Allergy Clin. Immunol.* **2013**, *68*, 261–273, doi:10.1111/all.12088.
32. White, J.; Dubey, S. Eosinophilic Granulomatosis with Polyangiitis: A Review. *Autoimmun. Rev.* **2023**, *22*, 103219, doi:10.1016/j.autrev.2022.103219.
33. Singh, D.; Bafadhel, M.; Brightling, C.E.; Sciurba, F.C.; Curtis, J.L.; Martinez, F.J.; Pasquale, C.B.; Merrill, D.D.; Metzdorf, N.; Petruzzelli, S.; et al. Blood Eosinophil Counts in Clinical Trials for Chronic Obstructive Pulmonary Disease. *Am. J. Respir. Crit. Care Med.* **2020**, *202*, 660–671, doi:10.1164/rccm.201912-2384PP.
34. Balzano, G.; Stefanelli, F.; Iorio, C.; De Felice, A.; Melillo, E.M.; Martucci, M.; Melillo, G. Eosinophilic Inflammation in Stable Chronic Obstructive Pulmonary Disease: Relationship with Neutrophils and Airway Function. *Am. J. Respir. Crit. Care Med.* **1999**, *160*, 1486–1492, doi:10.1164/ajrccm.160.5.9810105.
35. Kolsum, U.; Damera, G.; Pham, T.H.; Southworth, T.; Mason, S.; Karur, P.; Newbold, P.; Singh, D. Pulmonary Inflammation in Patients with Chronic Obstructive Pulmonary Disease with Higher Blood Eosinophil Counts. *J. Allergy Clin. Immunol.* **2017**, *140*, 1181-1184.e7, doi:10.1016/j.jaci.2017.04.027.
36. Lacoste, J.Y.; Bousquet, J.; Chanez, P.; Van Vyve, T.; Simony-Lafontaine, J.; Lequeu, N.; Vic, P.; Enander, I.; Godard, P.; Michel, F.B. Eosinophilic and Neutrophilic Inflammation in Asthma, Chronic Bronchitis, and Chronic Obstructive Pulmonary Disease. *J. Allergy Clin. Immunol.* **1993**, *92*, 537–548, doi:10.1016/0091-6749(93)90078-T.
37. Dai, C.; Yao, X.; Gordon, E.M.; Barochia, A.; Cuento, R.A.; Kaler, M.; Meyer, K.S.; Keeran, K.J.; Nugent, G.Z.; Jeffries, K.R.; et al. A CCL24-Dependent Pathway Augments Eosinophilic Airway Inflammation in House Dust Mite-Challenged Cd163 -/- Mice. *Mucosal Immunol.* **2016**, *9*, 702–717, doi:10.1038/mi.2015.94.
38. Chistiakov, D.A.; Killingsworth, M.C.; Myasoedova, V.A.; Orekhov, A.N.; Bobryshev, Y. V. CD68/Macrosialin: Not Just a Histochemical Marker. *Lab. Investig.* **2017**, *97*, 4–13, doi:10.1038/labinvest.2016.116.
39. Kwiecień, I.; Rutkowska, E.; Raniszewska, A.; Rzeszotarska, A.; Polubiec-Kownacka, M.; Domagała-Kulawik, J.; Korsak, J.; Rzepecki, P. Flow Cytometric Analysis of Macrophages and Cytokines Profile in the Bronchoalveolar Lavage Fluid in Patients with Lung Cancer. *Cancers (Basel).* **2023**, *15*, doi:10.3390/cancers15215175.
40. St-Laurent, J.; Turmel, V.; Boulet, L.P.; Bissonnette, E. Alveolar Macrophage Subpopulations in Bronchoalveolar Lavage and Induced Sputum of Asthmatic and Control Subjects. *J. Asthma* **2009**, *46*, 1–8, doi:10.1080/02770900802444211.
41. Chung, Y.; Hong, J.Y.; Lei, J.; Chen, Q.; Bentley, J.K.; Hershenson, M.B. Rhinovirus Infection Induces Interleukin-13 Production from CD11b-Positive, M2-Polarized Exudative Macrophages. *Am. J. Respir. Cell Mol. Biol.* **2015**, *52*, 205–216, doi:10.1165/rcmb.2014-0068OC.

 doi:10.20944/preprints202508.0471.v1

42. Sun, Y.; Liou, B.; Chu, Z.; Fannin, V.; Blackwood, R.; Peng, Y.; Grabowski, G.A.; Davis, H.W.; Qi, X. Systemic Enzyme Delivery by Blood-Brain Barrier-Penetrating SapC-DOPS Nanovesicles for Treatment of Neuronopathic Gaucher Disease. *EBioMedicine* **2020**, *55*, doi:10.1016/j.ebiom.2020.102735.
43. Papachristoforou, E.; Ramachandran, P. Macrophages as Key Regulators of Liver Health and Disease. In; 2022; pp. 143–212.
44. Lepekha, L.N.; Erokhina, M.V.; Demyanenko, N.G.; Shcherbakova, E.A.; Ergeshov, A.E. Macrophage Phenotypic Plasticity during Inflammation in Patients with Pulmonary Sarcoidosis or Tuberculosis. *Вестник Цниит* **2022**, 7–21, doi:10.57014/2587-6678-2022-3-7-21.
45. Vasconcelos, J.F.; Teixeira, M.M.; Barbosa-Filho, J.M.; Agra, M.F.; Nunes, X.P.; Giulietti, A.M.; Ribeiro-dos-Santos, R.; Soares, M.B.P. Effects of Umbelliferone in a Murine Model of Allergic Airway Inflammation. *Eur. J. Pharmacol.* **2009**, *609*, 126–131, doi:10.1016/j.ejphar.2009.03.027.
46. Lepekha, L.N.; Erokhina, M. V. Pulmonary Macrophages and Dendritic Cells. *Респираторная Медицина Руководство В 4 Т. 3-Е Изд., Доп. И Перераб. Т. 1.* **2024**, 249–263, doi:10.18093/987-5-6048754-9-0-2024-1-249-263.
47. Zlotnikov, I.D.; Ezhov, A.A.; Ferberg, A.S.; Krylov, S.S.; Semenova, M.N.; Semenov, V. V.; Kudryashova, E. V. Polymeric Micelles Formulation of Combretastatin Derivatives with Enhanced Solubility, Cytostatic Activity and Selectivity against Cancer Cells. *Pharmaceutics* **2023**, *15*, 1613, doi:10.3390/pharmaceutics15061613.
48. Ge, Z.; Chen, Y.; Ma, L.; Hu, F.; Xie, L. Macrophage Polarization and Its Impact on Idiopathic Pulmonary Fibrosis. *Front. Immunol.* **2024**, *15*, doi:10.3389/fimmu.2024.1444964.
49. Robbe, P.; Draijer, C.; Borg, T.R.; Luinge, M.; Timens, W.; Wouters, I.M.; Melgert, B.N.; Hylkema, M.N. Distinct Macrophage Phenotypes in Allergic and Nonallergic Lung Inflammation. *Am. J. Physiol. Cell. Mol. Physiol.* **2015**, *308*, L358–L367, doi:10.1152/ajplung.00341.2014.
50. Herold, S.; Mayer, K.; Lohmeyer, J. Acute Lung Injury: How Macrophages Orchestrate Resolution of Inflammation and Tissue Repair. *Front. Immunol.* **2011**, *2*, doi:10.3389/fimmu.2011.00065.